ENLIGHTEN
GEOSCIENCE LTD.

Induced Seismicity Study in the Kiskatinaw Seismic Monitoring and Mitigation Area, British Columbia

for the BC Oil and Gas Commission

Amy D. Fox, Ph.D., P. Geo. and Neil D. Watson, P. Geol.

Final Report

June 5, 2019

Disclaimer

All work performed for this project and information provided in this report is of the highest technical quality possible given data limitations and uncertainties at the time the work was completed. Enlighten Geoscience Ltd. cannot guarantee the accuracy of the material included in this report (and corresponding presentation) and bears no responsibility for the use of the material.

This report was written as a preliminary contribution to understanding issues surrounding induced seismicity in the Kiskatinaw Seismic Monitoring and Mitigation Area. The ability to predict induced seismicity or infer economic valuations is explicitly not meant to be implied from this report.

Enlighten Geoscience Ltd.

APEGA Permit P13351

PROFESSIONAL GEOSCIENTIST ALBERTA
AMY D. FOX

Member #159887

June 5, 2019

© 2019 Enlighten Geoscience Ltd.

Executive Summary

Induced seismicity has been a growing concern throughout North America and around the world as increasing numbers of seismic events have been occurring in historically quiet tectonic areas and appear to be related to localized oil and gas development activity. On November 29, 2018 hydraulic fracture operations were suspended after a series of three seismic events ranging from 3.4 to 4.5 magnitude were recorded in the Kiskatinaw Seismic Monitoring and Mitigation Area (KSMMA) in northeast British Columbia, Canada.

The goal of this study was to perform the first phase of a larger investigation designed to identify key or common factors coincident with induced seismicity and/or to delineate areas of higher induced seismicity likelihood within the KSMMA. The results of this and anticipated subsequent studies may be used in the development of standardized pre-assessment methodologies and inform potential mitigation protocols. The study was primarily an exercise of proprietary data collation, standardization and quality control/assurance with a limited structural geology, hydrodynamics and geomechanical interpretation.

The KSMMA has experienced structural activity from the Precambrian through to the current day. The Peace River Arch (a significant topographic high likely uplifted along reverse faults) influenced sedimentation patterns until the Early Carboniferous. The Peace River Arch began to collapse by way of normal faulting from the Early Carboniferous through to the end of the Permian. Strike-slip faulting became the dominant source of deformation during the Triassic. The Jurassic saw the onset of the Columbia Orogeny and this associated compression during the Jurassic resulted in the conversion of pre-existing structures to a transpressional setting. The Laramide Orogeny reintroduced a phase of compression and further fault reactivation. Isostatic rebound, estimated to be as high as 4 mm/year in the study area, related to the removal of up to 3 kilometres of overburden during the Laurentide Glaciation has been the primary tectonic influence in the Quaternary.

The development of a comprehensive hydrodynamic model was a key part of this study. The findings include the potential presence of several pressure terranes within the Upper and Middle Montney. These terranes illustrate the transition from relatively high over-pressuring to lower levels of over-pressuring to normal and sub-normal pressure regions. The Debolt through Belloy interval was also evaluated, and this interval also displayed a pattern of pressure transitions.

The state of stress throughout much of the KSMMA at depths between the Doig and Belloy appears to be strike-slip and in a near critical state, meaning only small fluid pressure increases are sufficient to cause specific sets of fractures and faults to become critically stressed. It is generally believed that critically stressed faults are a key factor in induced seismicity. The amount of pressure increase needed is closely tied to the existing formation pressure – areas with higher natural pressures require no or low pressure increases. Fractures/faults that will become critically stressed first, if they exist, strike approximately 15° to 45° from the northeast-southwest maximum horizontal stress orientation and are dipping more than 60°. Further study is needed to better understand both the state of stress and the distribution of existing faults and fractures in the KSMMA, as well as the implications of the discrepancy between the known seismic events and the most critically stressed fracture/fault orientations.

© 2019 Enlighten Geoscience Ltd.

Although access to data, as well as data quality, remain key challenges in the study area, most data is available in the public domain. Data accessibility and quality has been addressed in each of the report sections and in the report summary. Work is on-going to address all data-related issues. Once resolved, it will take significantly more time and expertise to fully analyze all available data.

Contents

© 2019 Enlighten Geoscience Ltd.

I. Introduction

Induced seismicity has been a growing concern throughout North America and around the world as increasing numbers of seismic events have been occurring in historically quiet tectonic areas and appear to be related to localized oil and gas development activity. In many parts of the world, e.g., the Groningen gas field in the Netherlands and the Ekofisk field in the North Sea, production-related seismicity has been experienced for decades and is relatively well-understood. More recently, however, there has been an increase in injection-related seismicity, particularly in tight, unconventional reservoirs. Originally linked to high volumes of water injection for disposal purposes, it is now clear that at least some of the seismicity in certain areas is being caused by well completions, particularly multi-stage hydraulic fracturing of horizontal wells (e.g., Kozlowska et al., 2018, Ngo et al., 2019).

The mechanism behind injection-induced seismicity is generally considered to be slip on pre-existing faults that are put into a critically stressed state. Factors necessary to explain the occurrence of such events includes knowledge of pre-existing faults (locations, orientations, sizes, frictional properties) as well as in situ stresses and pressures (original and induced changes) in the subsurface. Having a good understanding of these factors can be extremely helpful in deciphering where and why induced seismic events occur (Lund Snee and Zoback, 2018), which then may help identify mitigation approaches.

Kiskatinaw Seismic Monitoring and Mitigation Area

Monitoring for induced seismicity has been a priority in British Columbia (BC) since the early 2010's when the BC Seismic Research Consortium was established to expand the capability of the Canadian National Seismic Network in northeast BC. In 2015, regulatory enhancements to the drilling and production regulations were put into force to oversee induced seismicity. The Kiskatinaw Seismic Monitoring and Mitigation Area (KSMMA) was established in the greater Farmington area of British Columbia with the issuance in May 2018 of a Special Project Order by the BC Oil and Gas Commission (OGC). The order required operators in the defined area to provide substantial technical due diligence prior to, during and after hydraulic fracturing operations and was in response to concerns about induced events linked to the development of the Triassic Montney play (OGC, May 2018). Requirements laid out in the Special Order included, but were not limited to, a pre-assessment of seismic hazard, real-time seismic monitoring (with defined thresholds) during fracturing operations and post-job reporting.

On November 29, 2018 hydraulic fracture operations at a Canadian Natural Resources Ltd. (CNRL) well pad were suspended after a series of three seismic events ranging from 3.4 to 4.5 magnitude were recorded. There were 14 associated reports of felt events at the surface, and an active BC Hydro construction site was evacuated as a precautionary measure. After an investigation by the OGC, it was concluded that the events were indeed caused by fluid injection during CNRL's hydraulic fracturing operations in the Middle Montney.

The requirements in the May 2018 Special Order have been met by the KSMMA operators using a variety of approaches, and, as such, geologic and seismic data collected by them varies significantly. The lack of consistency in type, quantity and quality of data being collected, and especially in data that has been collected in the past, makes it difficult to develop a good understanding of the induced seismicity in the region.

© 2019 Enlighten Geoscience Ltd.

Some of the most critical, currently unanswered questions in the KSMMA include:

- Where is seismicity likely to occur, and why does it appear to vary both across the KSMMA and stratigraphically?
- Are some of the events occurring outside of the Montney formation, for example in the underlying Belloy formation, which is normally to moderately under-pressured relative to the local hydrostatic gradient?
- Why do most completion (hydraulic fracturing) activities have no events?
- Why do some completions induce many, smaller events while others seem to induce less frequent but larger events?
- What is the role of structure?
- What are the pressure communication mechanisms in the subsurface, and how do they relate to the seismic events?
- What are in situ stresses in the KSMMA, and can knowledge of them be used to assess induced seismicity risk?
- What is the distribution of pre-existing faults in the subsurface, and which ones are most susceptible to induced slip?
- Are there specific operational parameters (e.g., pumping volumes or rates) that can be optimized to reduce the risk of induced seismic events during hydraulic fracturing operations?

Project Goals and this Report

The OGC's objective is to identify key or common factors coincident with induced seismicity in the KSMMA and delineate areas of higher occurrence within the KSMMA to aid in the development of standardized pre-assessment methodologies and mitigation protocols. The goal of this study was for Enlighten Geoscience Ltd. (Enlighten) to act as an objective, nonpartisan third party (neither regulator nor operator) and perform the first phase of a larger investigation designed to achieve the OGC's objective. It was anticipated that this project would primarily be an exercise of proprietary data (from the KSMMA operators) collation, standardization and quality control/assurance with a limited, preliminary interpretation. However, given the large quantity of public data available (see section II), a significant amount of structural, hydrodynamic and geomechanical interpretation was possible, and the findings are presented in this report. Also included in the various discussions, and summarized at the end of this report, are numerous recommendations for further work.

Note that several of the figures in the report, particularly the maps, are available as larger-scaled figures or enclosures in Appendix C.

Study Area

The KSMMA, as defined by the OGC, is illustrated in Figure 1. The study area for this project extends from T. 76, R. 12 W6 to T. 86, R. 23 W6. This extension beyond the KSMMA boundaries allows the inclusion of a regional context to the evaluation, particularly the structural geology and hydrodynamics.

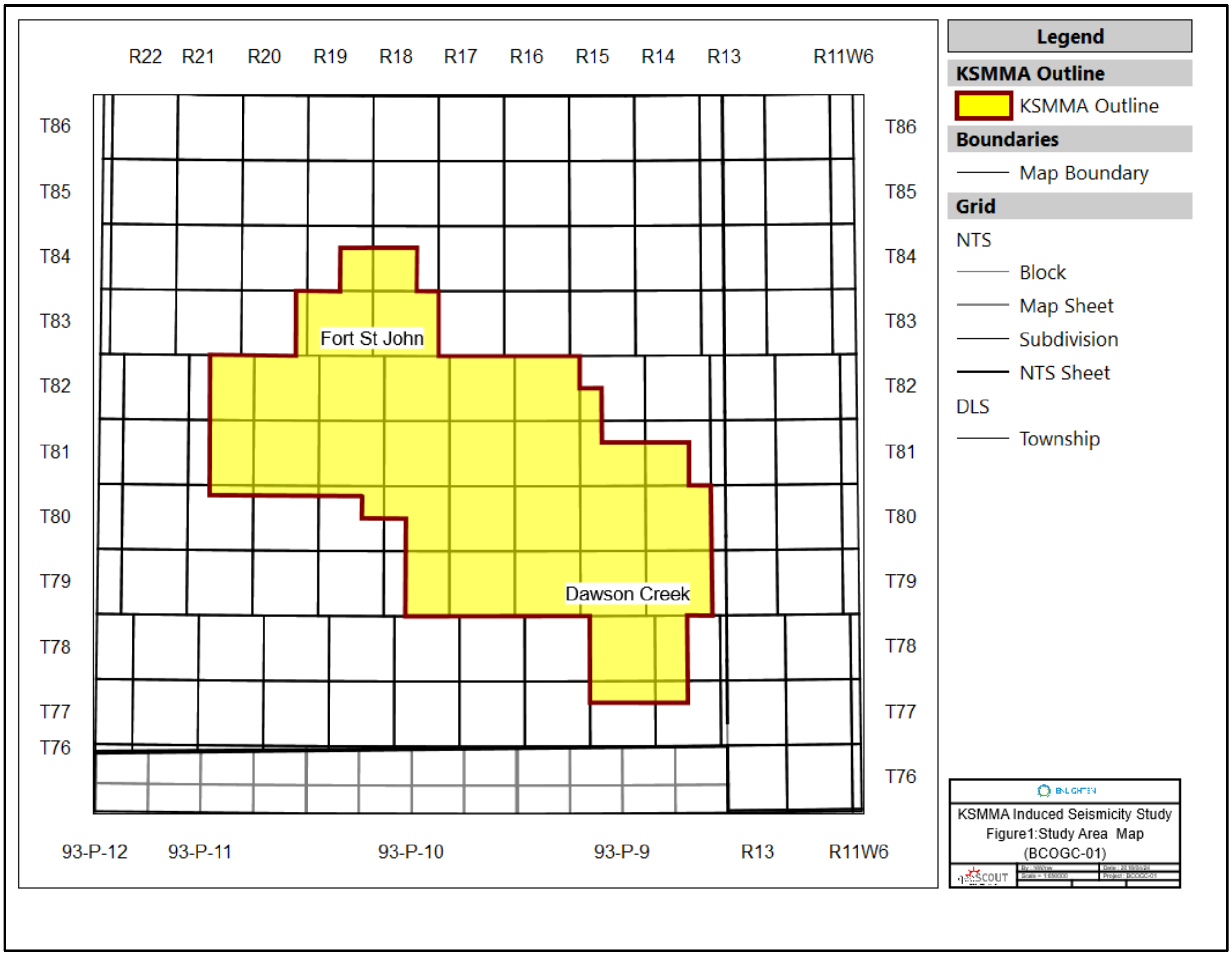

Figure 1. The study area with the KSMMA in yellow.

Confidentiality and Operator Aliases

During this project, Enlighten personnel and sub-contractors were given access to certain operator confidential information, including viewing seismic data and structural interpretations. While specifics of this data are not discussed in this report, where necessary for clarity, reference will be made to general observations regarding the confidential information. In order to maintain confidentiality of the data, each of the six participating operators has been assigned a randomly assigned alias letter (A through F) when discussing these observations.

All the operators have near-field seismic monitoring equipment. Enlighten incorporated Moment Tensor data greater than magnitude 1.5 from a selection of this dataset, for interpretation, but the data were not made available for inclusion in the project deliverables.

Fault Nomenclature

Reference will be made throughout this report to various modes of failure and faulting. For the purposes of this report, faults are classified as follows (after Ragan, 1973 and USGS 2019a):

- Dip-slip: Fault where the primary movement is along the dip plane.

    - Normal Fault: Dip-slip fault where the Hanging Wall has moved down relative to the Foot Wall. Typical of extensional deformation.
    - Reverse Fault: Dip-slip fault where the hanging Wall has moved upwards relative to Foot Wall. Typical of compressional deformation.
    - Thrust Fault: Reverse fault with dip <45° with considerable crustal shortening. While often used interchangeably with Reverse Fault, the distinction is important when contrasting deformation between thrust dominated Foothills regions and non-Foothills regions.
    - Growth Fault: Normal fault with syn-sedimentary deformation resulting in thickened stratigraphic thickness along the Hanging Wall of the fault.
- Strike-slip: Fault where the primary movement is along the strike plane.
    - Wrench Fault: A style of Strike-Slip Faulting in which the fault plane is essentially vertical.
    - Transpression: Strike-Slip faulting modified by crustal shortening.

II. Project Data

Data Sources

geoSCOUT™

Enlighten used geoSCOUT software for data searching and mapping. geoSCOUT was particularly important for finding wells with pressure data, core and public image logs.

OGC

The OGC well files, accessible online, were an important source for high-quality public image logs (many with fracture interpretations) and two fracture studies in the Doig and Montney. Several wells with white-light core photos (slab or whole) were found by physically checking the OGC well file for every well that collected core from the Doig to the Montney.

Petro Ninja and the Alberta Energy Regulator

Petro Niche Technologies Ltd. is a Calgary-based company that has developed a map-based oil and gas well information platform called Petro Ninja. Enlighten partnered with Petro Niche to add data to Petro Ninja from several Alberta Energy Regulator databases including the Reservoir Evaluation and Productivity Studies Index and Geological and Other Studies Index. Petro Niche then created a dashboard-based search engine to find specific data types within these databases. This data source was particularly important for locating mechanical tests on core in the Doig, Montney and Belloy. Although the data are outside of the KSMMA area, they were used along with operator-provided data and limited core test data from the OGC database to determine the most appropriate equations for calculating rock properties from well logs.

Operators

The KSMMA operators provided some of their own data, primarily minifrac tests and/or test results, image logs and triaxial tests. Data found in the OGC database or using geoSCOUT are considered public even if they were also provided by a KSMMA operator. Data available only through the operators is considered proprietary and was used for interpretation but is not included in any way in this report or any other project deliverables.

Seismic Data

A summary of the seismic data quality and structural interpretation review has been included as Appendix A – KSMMA Geophysical Review.

Minifrac (DFIT) Data

A summary of the minifrac review has been included as Appendix B – KSMMA Minifrac Review.

III. Stratigraphic Model

Prior to this report, earthquakes deemed to be induced seismic events caused by hydraulic fracturing in the Montney were assigned to either the Upper Montney or Lower Montney. It was the initial intention for this study to continue using this terminology, but it quickly became apparent that this would be unworkable given variations in the applications in this terminology between operators.

Recently published research (i.e., Davies et al., 2018; Euzen et al., 2018; Moslow et al., 2018; Zonneveld and Moslow, 2018) established a consistent and agreed upon primary sub-division of the Montney into Upper, Middle and Lower Montney. These subdivisions are consistent with the global Triassic sub-stages. This stratigraphic framework is illustrated in Figure 2 (T. Euzen, personal communication). Data and interpretations in this study are presented in the context of this framework.

© 2019 Enlighten Geoscience Ltd.

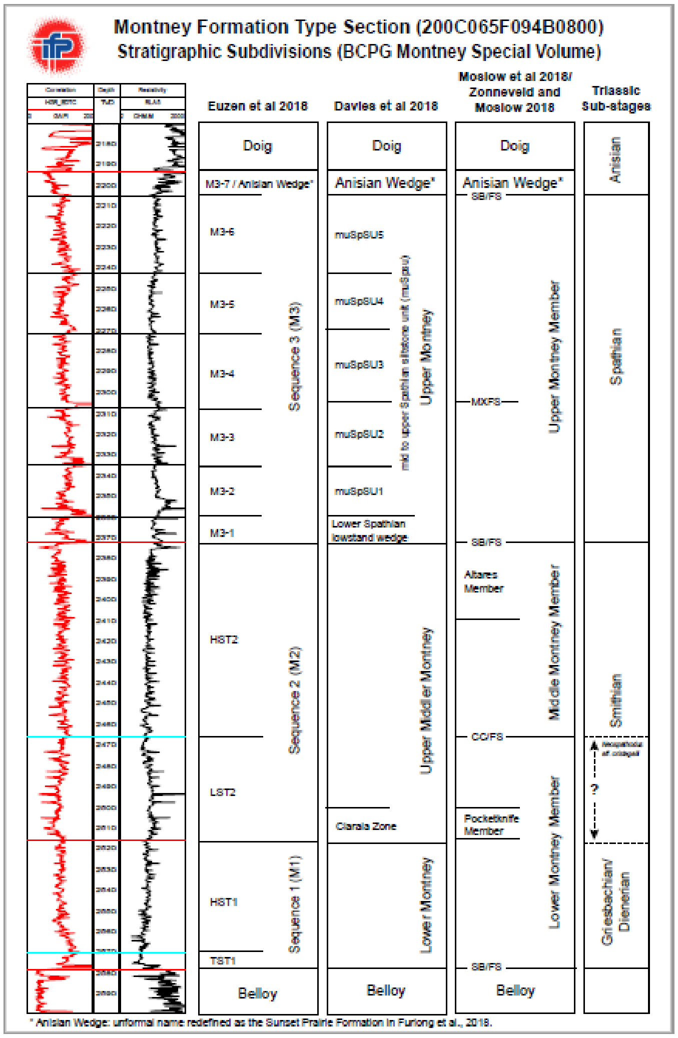

Figure 2. Montney Formation type section.

IV. Tectonic History and Structural Setting of the KSMMA and Surrounding Area

Crustal Geology

Basement Terranes

The KSMMA area overlies the north – south trending contacts of three Basement Terranes of varying ages (Ross et al., 1994). These terranes are, from east to west, the Ksituan (Proterozoic), Kiskatinaw (Age unknown) and Slave Lake (Archean). Figure 3 illustrates the distribution of basement terranes relative to the KSMMA. These terranes are subject to brittle as opposed to ductile deformation (Burwash et al., 1994) in that they are more likely to fracture and fault than fold when subjected to increasing stress.

© 2019 Enlighten Geoscience Ltd.

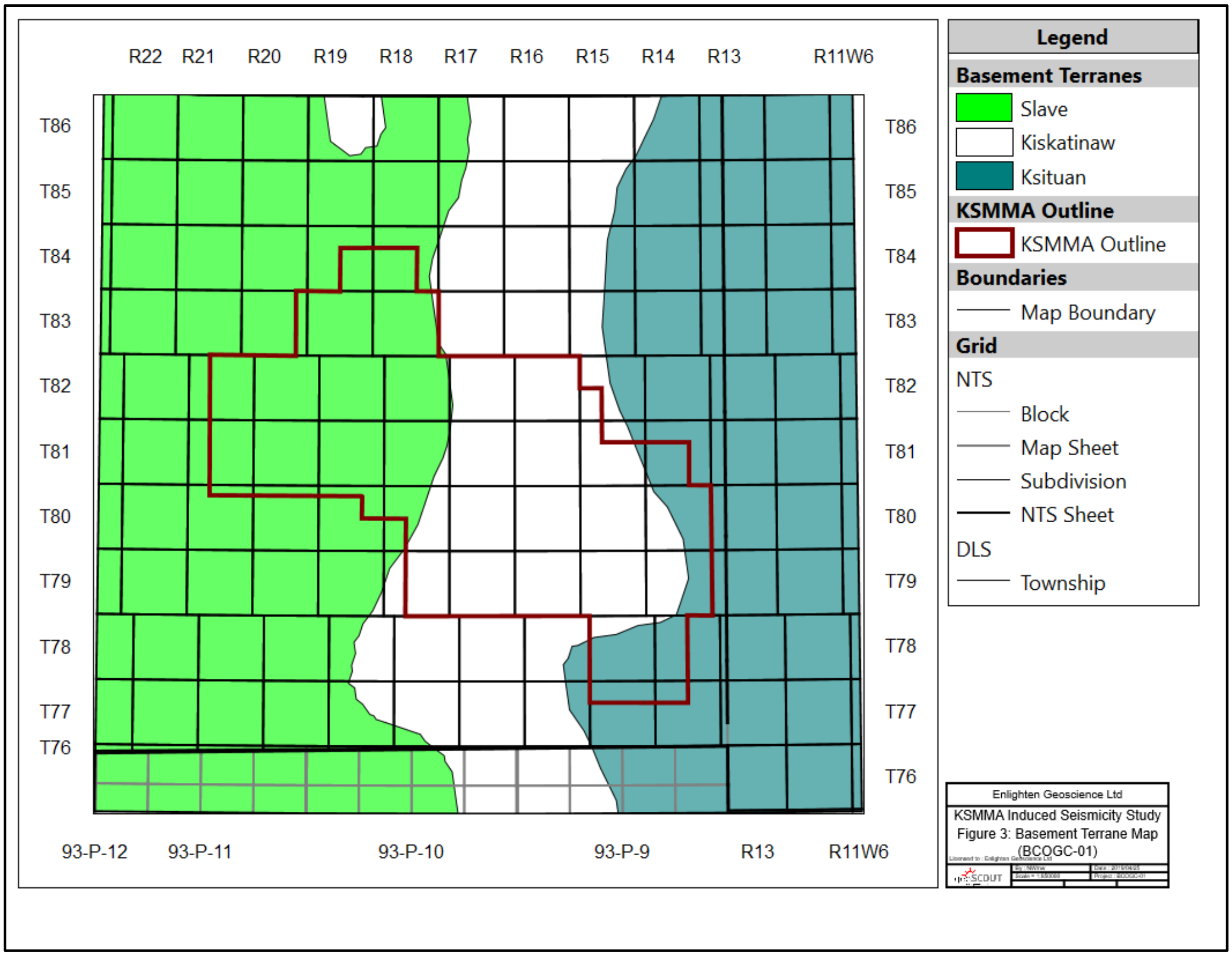

Figure 3: Map of basement terranes within study area.

Precambrian to Carboniferous

Development of Peace River Arch During the Proterozoic

The Peace River Arch (PRA) was uplifted during the Proterozoic and remained a structurally positive element influencing sedimentation through the early-most Carboniferous (O'Connell, 1994) as illustrated in Figure 4. Although the origins are of the PRA are unclear, it represents the longest-term tectonic feature in the Western Canada Sedimentary Basin.

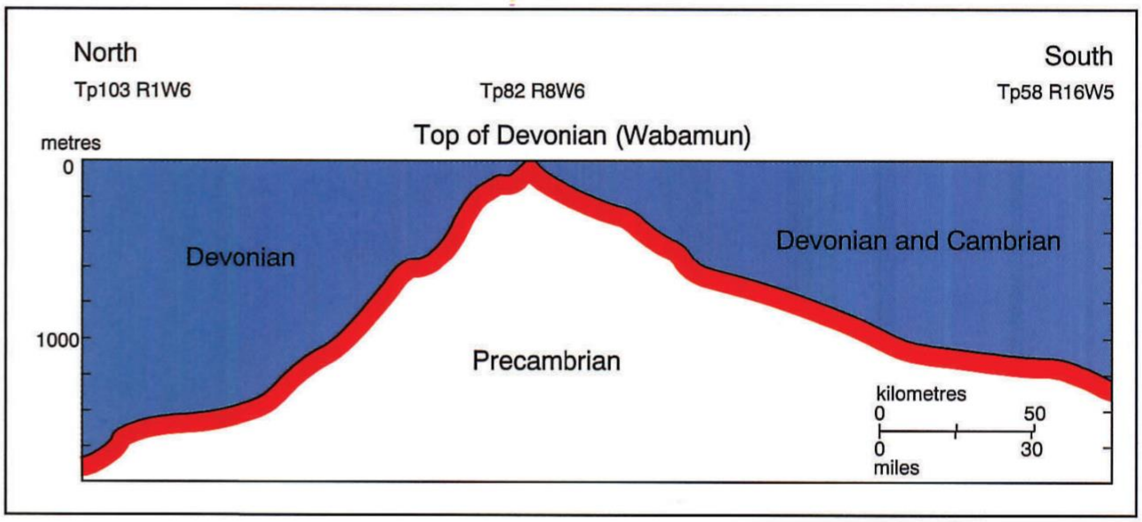

Figure 28.3 North-south cross section across the Peace River Arch from the top of the Devonian to the top of the Precambrian. The location of the section is shown in Figure 28.4. Vertical exaggeration is 58:1.

Figure 4. Schematic north-south cross section over Peace River Arch (O'Connell, 1994).

Preliminary Collapse of PRA During Pekisko Through Debolt Time

From the Earliest Carboniferous onwards, the Peace River Arch began to collapse through a series of normal faults and form the Peace River Embayment. These faults show evidence of continued reactivation and modification from Pekisko time to the Recent.

O'Connell (1990) outlined syn-tectonic depositional and isopach changes in the Banff and Pekisko Formations of the Rundle Group. Although his mapping is truncated at the Alberta – British Columbia Boundary, the text indicates that these trends continue into BC.

Further faulting was manifested during the formation of the Debolt. Evidence of growth faulting during the Debolt was observed by G. Davies (personal communication), as illustrated in Figure 5. This style of deformation was observed to have occurred in the KSMMA during the seismic review provided by Operator C.

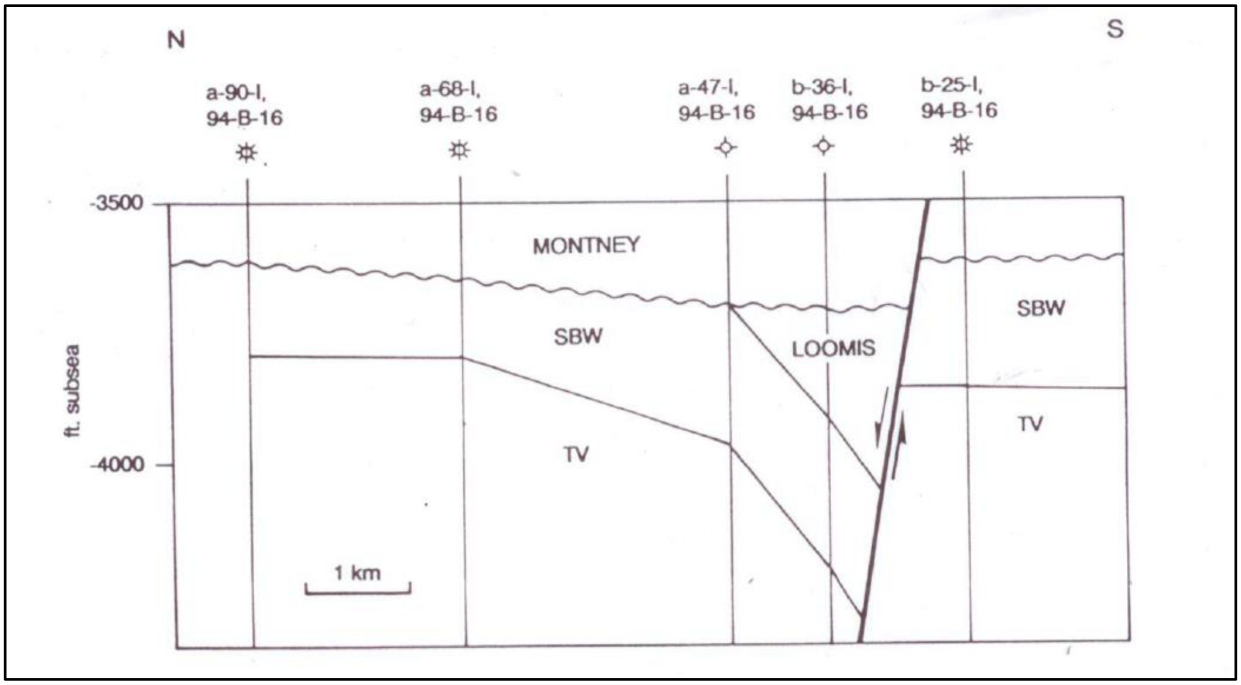

Figure 5. Illustration of Debolt growth faulting (GDGC and Hamid Majid, 1990).

Formation of Dawson Creek Graben Complex

The most widely recognized structural event in the KSMMA was the development of the Dawson Creek Graben Complex (Barclay et al., 1990), which refers to the depocentre created by the syn-sedimentary final major phase of Peace River Arch collapse beginning at the end of Mississippian Debolt time and continuing through the Permian Belloy Formation. This is schematically illustrated in Figure 6.

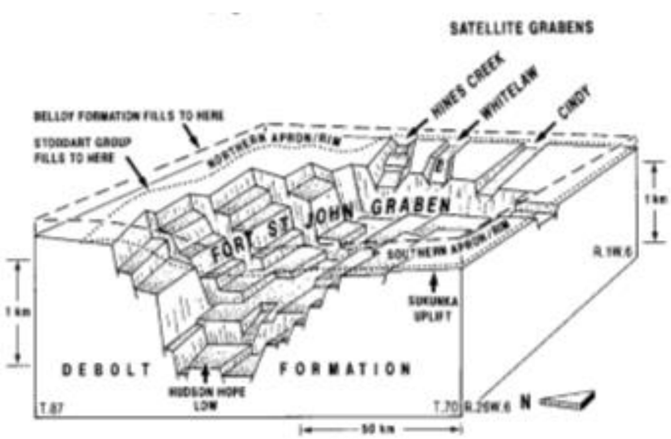

Fig. 9. Sketch of Carboniferous-Permian Dawson Creek Graben Complex. Golata, Kiskatinaw, Taylor Flat, and Belloy formations successively filled the graben complex as it developed. The reconstruction shows arcuate shape, wedge-like westward deepening, and internal and satellite grabens and horsts. Sketch is based on cross-sections, and on isopach and structure maps.

Figure 6. Sketch of the Ft. St. John Graben (Barclay et al., 1990).

Structural Influence on Montney and Doig Deposition

The Montney generally records basin fill influenced by paleostructures. Penecontemporaneous movement or structuring appears to have been minimal in the KSMMA, although the Hay River Fault Zone to the north of the KSMMA and other events appear to have influenced aspects of Middle Montney deposition (Davies et al., 2018).

Dixon (2011) linked syn-sedimentary faulting to the genesis of "Anomalously Thickened Sandstone Bodies" in the Doig formation including several examples within the KSMMA.

Fault Reactivation

Columbia to Laramide Compression and Reactivation to Transpression Regime

Numerous sources have recorded the influence of the Columbia and Laramide Orogenies reactivating the existing predominately normal faults into a transpressional tectonic setting (O' Connell, 1994).

In the Montney, all Operator seismic reviews provided examples of faulting that was generally interpreted as primarily consisting of faults that sole out in the lower Montney. Additional Operator interpretations and Enlighten observations include:

i. Riedel shears (Operators A and D in particular) indicative of the early stages of strike-slip deformation
ii. Flower structures (Operators B, C, E and F)
iii. Faults indicating significant post-Montney structuring either by a fault extending through the entire Montney or other faults causing anticlinal structures at the top of the Montney (Operator B)
iv. Possible thrust in North Pine evaporite (Operator C). Whether this is the result of thrust faulting or strike-slip duplexing remains to be determined.

Norgaard (1997) illustrated an example of structural inversion of Mississippian faults as a result of transpression beginning during the Jurassic and continuing through the post-Albian in a case study of the Monias Halfway Field. This review included an example of seismic expression of these structural features extending from Precambrian time through the Halfway and above. Figure 7 illustrates the location of the seismic line and the structural features creating the Monias Halfway Field. Similar structural inversion was recorded by Berger et al. (2009) as shown in Figure 8.

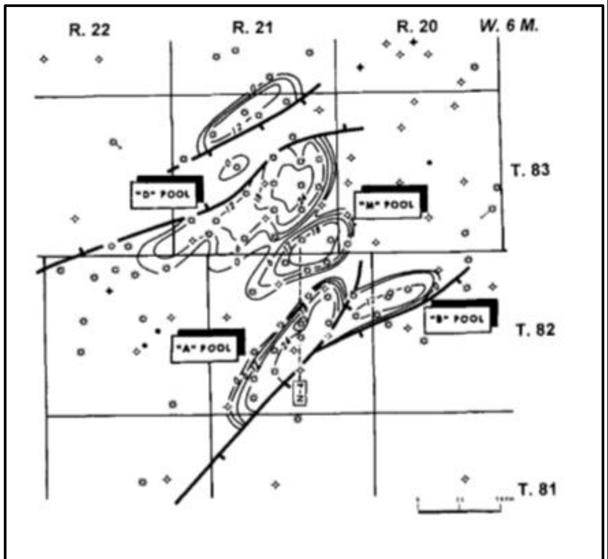

Fig. 8. Lower Halfway sandstone net gas pay Monias area with seismic line N-4 highlighted. Contour Interval = 6 m.

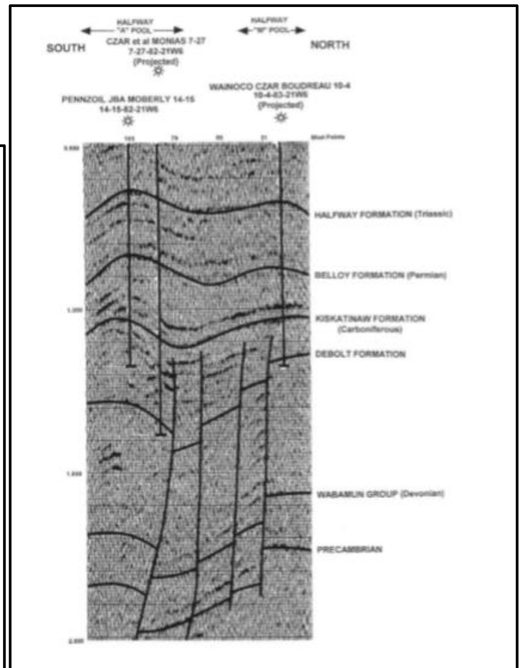

Fig. 9. Structure seismic section line N-4 (see location on Fig. 8). Inversion of the Halfway Formation possibly caused by reactivation of deep-seated early normal faults possibly due to strike slip movement associated with thrust faulting to the west.

(a) (b)

Figure 7. a) Seismic line of section, b) Interpreted seismic line.

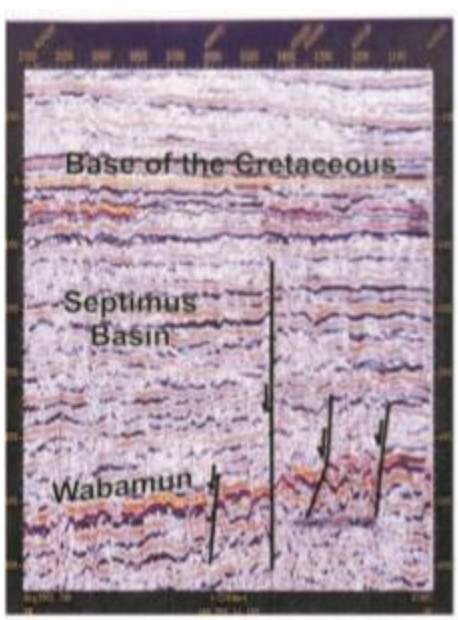

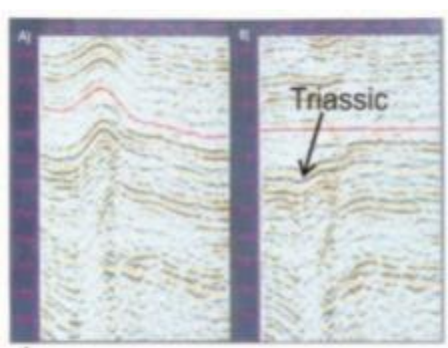

(a) (b)

Figure 8. Sample seismic sections across Septimus (a) and Monias features (b) from Berger et al., 2009.

Upper Cretaceous

Within the Upper Cretaceous, the influence of reactivated faults on Peace River Group and Lower Shaftesbury depositional trends was documented by Leckie et al. (1990).

Surface and Near-Surface Fault Expression

Berger et al. (2009) provided evidence of a connection between with modern hydrology within the KSMMA and Basement faults, as identified by High Resolution Aero-Magnetic data (Figure 9).

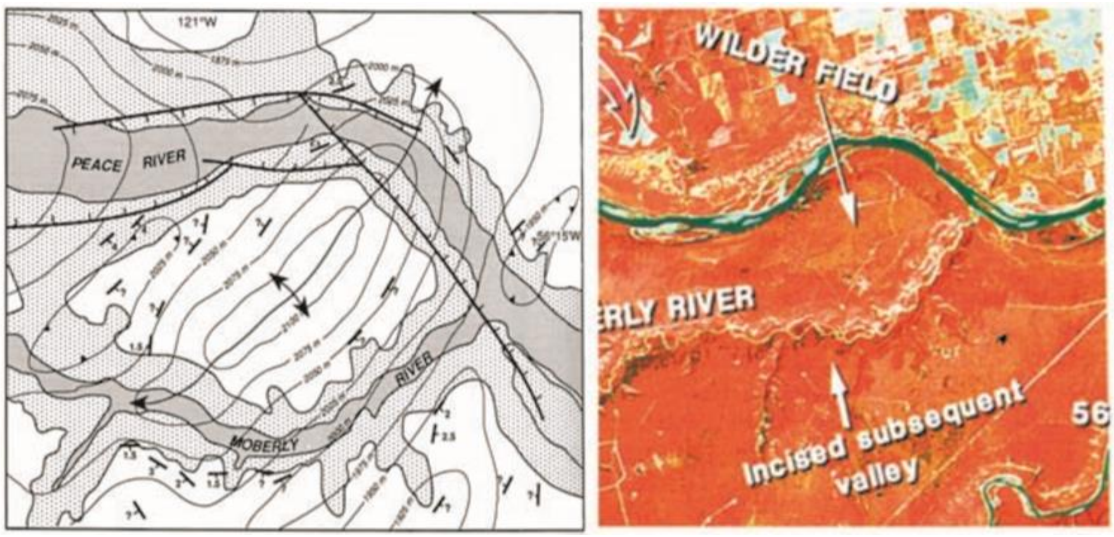

(a) (b)

Figure 9. Illustration of possible influence of basement faults on current hydrology (Berger et al., 2009)

Divergent Wrench Fault Zone

The assemblage of structures published in peer and non-peer reviewed literature illustrate the effect of a divergent wrench fault system on the KSMMA and surrounding area active from the Early Carboniferous through the present day. These observations are buttressed by the review sessions provided by the KSMMA Operators. Recently published examples of varying types of flower structures documented by Huang and Liu (2017) provide a useful classification for the structuring observed in the KSMMA.

Differential Erosion and Isostatic Rebound

Isostatic rebound related to the overburden and ice sheet removal towards the end of the Laurentide Glaciation is the final tectonic event that has influenced the structural setting of the KSMMA.

Up to 3 km of pre-Eocene deposits is estimated to have been removed by the Cordilleran Ice Sheet of the Laurentide Glaciation (Dawson, 1994). This overburden removal is in addition to the 3 km thickness of the Cordilleran Ice Sheet. As a result of this event, the KSMMA area has been undergoing significant isostatic rebound over the past approximately 20,000 years and is currently subject to significant vertical crust movement in the range of 3 to 5 mm/year (Koohzare et al., 2008) as shown in Figure 10.

A study of the New Madrid Fault Zone (located at the boundary between Missouri, Arkansas, Tennessee, and Kentucky) found that ice sheet loading suppressed seismicity and that subsequent unloading due to ice sheet removal enhanced seismicity in the region (Grollimund and Zoback, 2001). No mention was made of the impact of additional unloading due to erosion or whether the erosion is as significant as regions proximal to the Cordillera. The impact of crustal unloading due to Laurentide glaciation likely deserves further study.

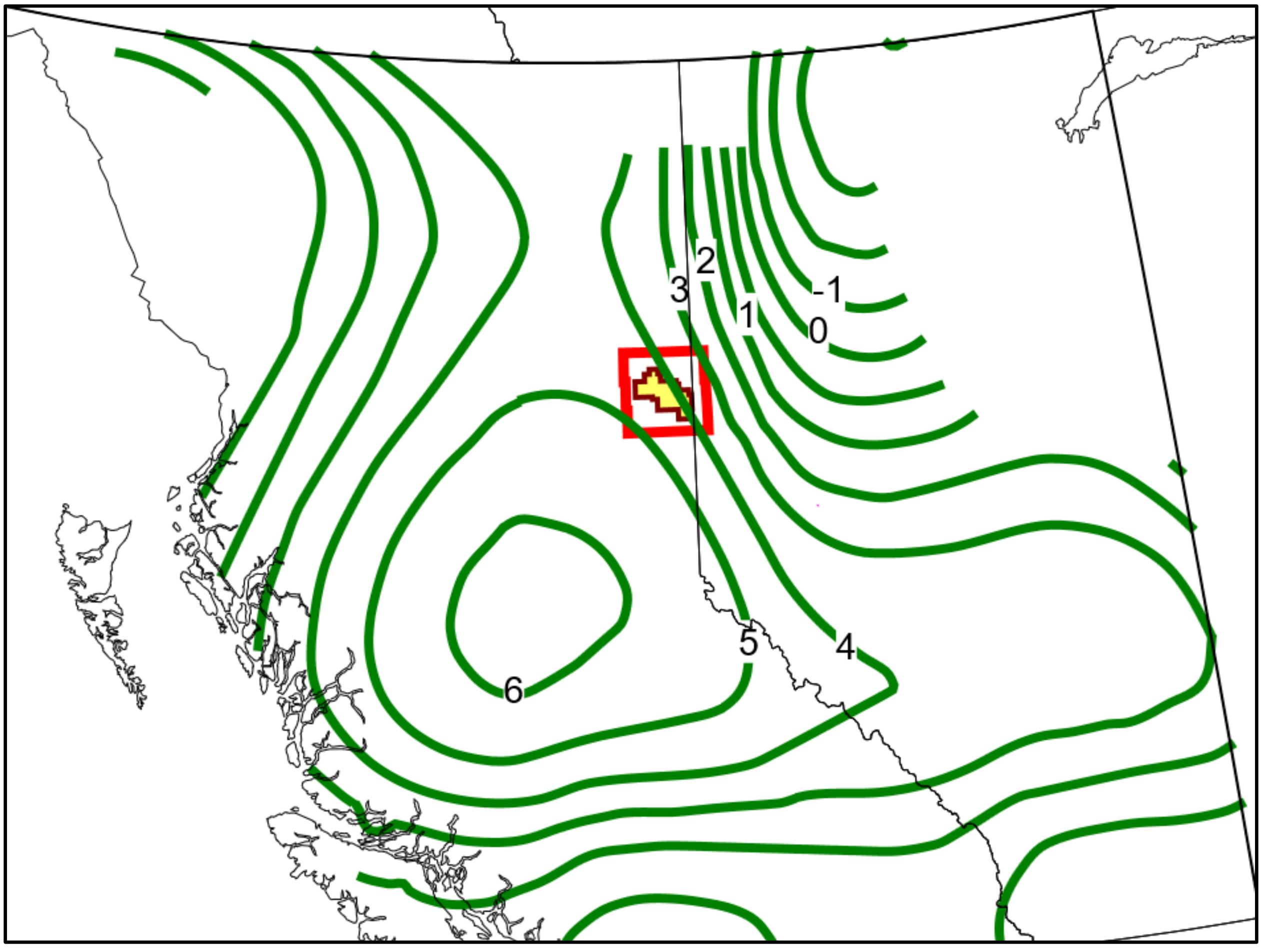

Figure 10. Vertical crustal movement contour map of western Canada and the 4 mm/year contour relative to the KSMMA (Koohzare et al., 2008).

Map of Fault Traces

Ample evidence exists that the KSMMA has been structurally active from the Precambrian through to the present day. A significant challenge for this study has been how to best represent this complex history for the understanding of induced seismicity.

The use of structural interpretations of the Montney and adjacent horizons based on high quality seismic data would have been the strongly preferred avenue for this purpose. Time and budget precluded the authors from utilizing these techniques for this preliminary study. Operators in the KSMMA have performed seismic interpretations and shared these on a confidential basis. The operators declined to allow these interpretations to be included in the report. The reasons given for withholding this important input included the need to protect asset valuations, exploration prospects and other concerns.

Fortunately, the KSMMA structuring has been the locale for a significant number of published interpretations. A composite map of faults in the study area was produced from the following sources:

i. Berger et al., 2009
ii. Davies et al., 2018 (after Berger, 2009)
iii. Hayes et al., 2015
iv. Norgaard, 1997
v. BC OGC Pool Breaklines Shapefiles

A map of compiled faults is shown in Figure 11. It should be noted that since these faults reflect a variety of mapping techniques and stratigraphic intervals, the precise location of some faults may vary from the map and not all faults may be identified. Fault dip can translate the position of a non-Montney level fault relative to Montney structures. This effect can be pronounced when basement level faults are considered given the isopach from between the Montney and the basement is 2 km or more. Another factor to consider when translating fault placement is deformation style. Listric faults (faults with a decreasing vertical displacement with depth) are an example of such a feature.

Geographic positioning of faults is another challenge. The Hayes et al. (2015) faults and OGC Pool Breaklines were derived from ESRI shapefiles and their positioning is, as a result, considered to be very accurate. Berger et al. (2009) and Norgaard (1997) faults were not available as shapefiles. In order to bring these features into the project maps, a technique known as georeferencing was applied. It is the experience of the second author that, in this process, it is best to use a map with abundant identifiable and precise (i.e. latitude and longitude) location markers. Where shapefiles are not available, the use of georeferenced images is preferred over other methods which do not account for differences in coordinate systems between the original map and the target map.

These faults are presented in the context of a preliminary interpretation of the KSMMA induced seismicity factors. The authors emphasize they not be used for any other purposes (i.e. asset valuations or risk assessment).

© 2019 Enlighten Geoscience Ltd.

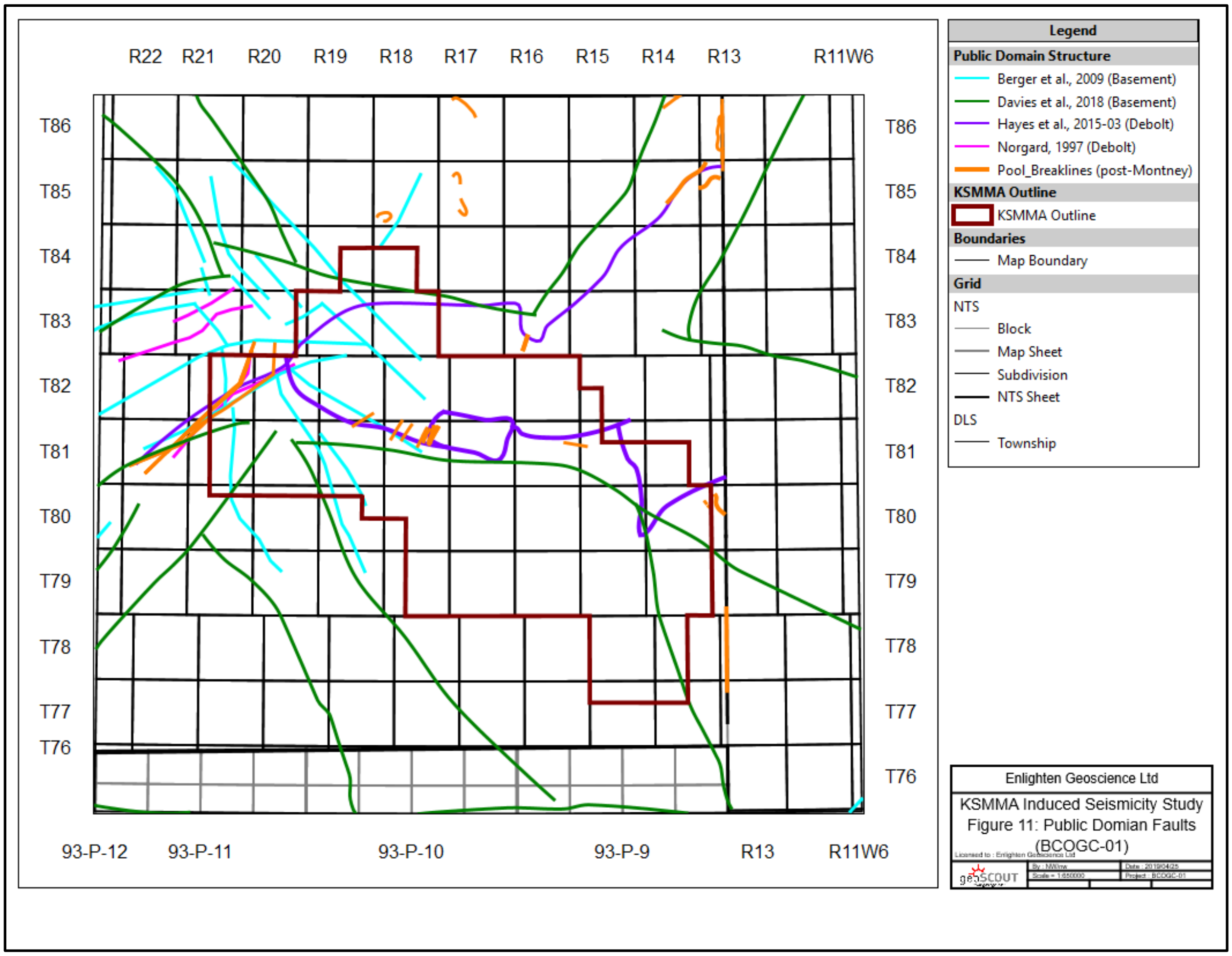

Figure 11. Map of faults derived from published sources. These faults reflect a variety of mapping techniques and stratigraphic intervals. As a result, the fault locations should be considered approximate.

The faulting discussed in this section represents very complex features. When viewed in outcrop, faults of this style are complex three-dimensional assemblages of en echelon smaller scale displacements, structural transfers and reactivations. Due to matters of scale and to maintain legibility, these faults are generally depicted by a line on a map or cross-section in which the inherent complexity is implicitly expressed. In a similar manner, any discussion of the influence of reactivated faults having an influence on modern day topographic features in no way implies the existence of a single fault extending from depth to surface.

The Earthquakes Canada (NRCan) seismic event catalogue data from January 20, 2010 through January 29, 2019 are displayed in Figure 12. Although these events are displayed on a separate figure for purposes of clarity, the correspondence to several features can be clearly discerned as discussed throughout this report.

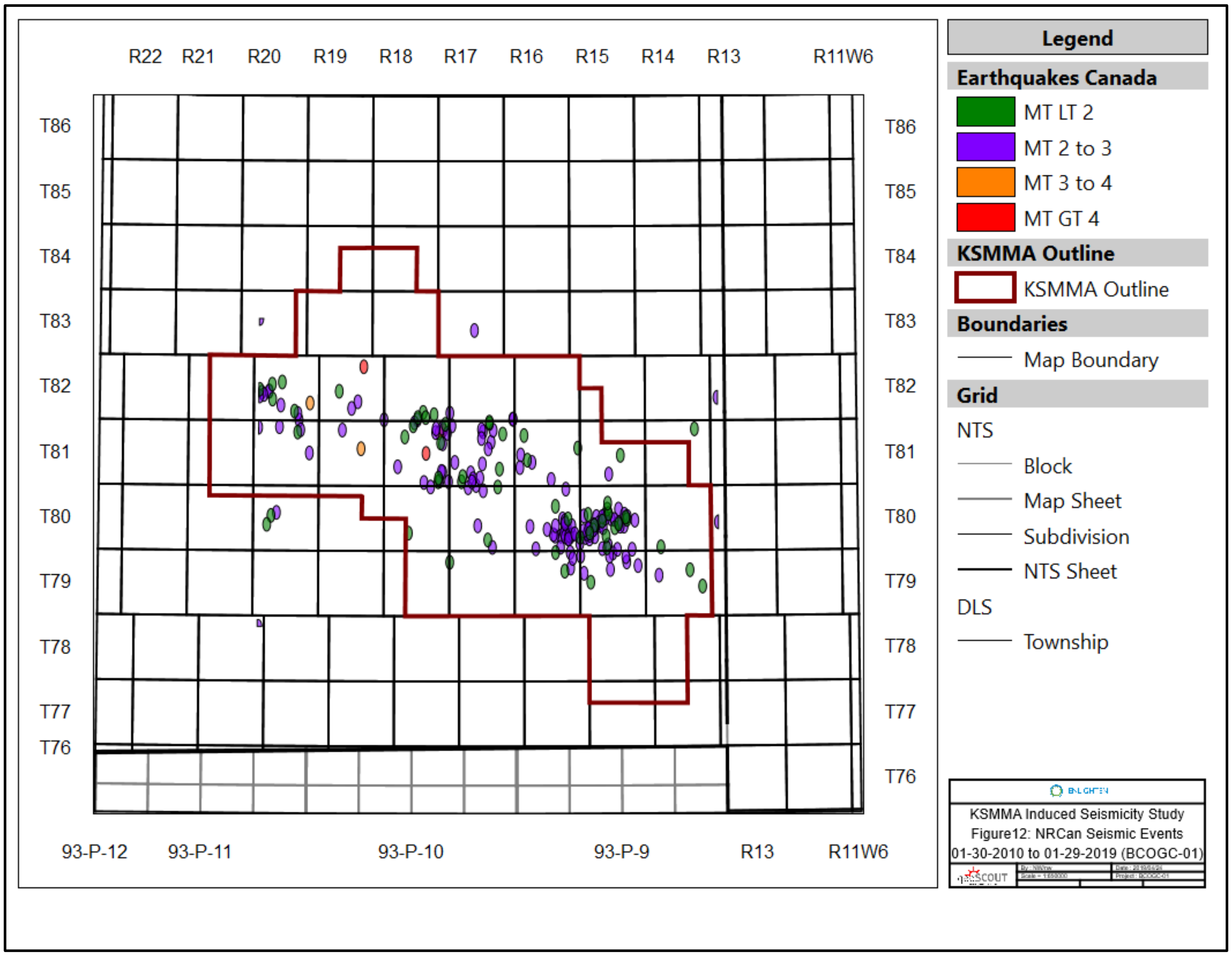

Figure 12. Map of NRCan Seismic Events from 01-30-2010 through 01-29-2019. Events are binned by magnitude.

V. Hydrodynamics

The hydrogeologic setting is considered one of the most important considerations in understanding induced seismicity. Not only are existing pore pressures important, but so is hydrologic communication potential (Walters et al., 2015). Because pressure data are relatively abundant in the public data sets, considerable effort was made in this study to not only map pressure throughout the study area, but also begin to define potential pressure compartments and understand where there is potential for hydraulic communication.

It is the experience of the authors that structural features can cause significant pressure compartmentalization in very low permeability plays (e.g. North Montney, Kaybob Duvernay, Willesden Green Duvernay and Delaware Basin Wolfcamp).

Data sourcing and Quality Control

All public domain pressure tests within the study area from the base of the Debolt to the top of the Triassic were identified and downloaded using geoSCOUT software. This yielded the following tests:

Pressure Test Type	Count
Drill Stem Tests (DSTs)	5,386
AB Completion Tests (AB AOFs)	1,802
BC Completion Tests (BC AOFs)	10,463
AB Oil Zone Pressures (OZPs)	1,773
Total Tests	19,424

Table 1. Summary of Debolt to Triassic all pressure tests.

The stratigraphic distribution of all pressure data for this project is highlighted in Table 2.

Stratigraphic Interval	DSTs	AB AOFs	BC AOFs	OZPs	Total Tests
Debolt	96	0	9	0	105
Stoddart	590	582	216	0	1388
Belloy	810	9	1051	7	1877
Lower Montney	52	8	21	0	81
Middle Montney	55	73	339	12	479
Upper Montney	49	23	1262	14	1348
Commingled Montney	0	0	11	0	11

Table 2. All pressure data distribution by stratigraphy and test class.

Only maps and plots key to outlining the hydrodynamic interpretation have been inserted into the body of the report. Other maps (e.g. Data Distribution) are listed in Table 3 and have been included as Enclosures in Appendix C.

Enclosure #	Enclosure Name
1	All Pressure Data Distribution Map
2	Debolt to Belloy - All Pressure Distribution Map
3	Lower Montney - All Pressure Distribution Map
4	Middle Montney - All Pressure Distribution Map
5	Upper Montney- All Pressure Distribution Map
6	Post Montney - All Pressure Distribution Map
7	All Pressure Data PE Plot
8	Debolt to Belloy - All Pressure Data PE Plot
9	Lower Montney - All Pressure Data PE Plot
10	Middle Montney - All Pressure Data PE Plot
11	Upper Montney - All Pressure Data PE Plot
12	Post Montney - All Pressure Data PE Plot

Table 3. Appendix C maps and plots not shown in this report.

All tests were subjected to stringent quality control (QC) evaluation to remove poor quality tests. The remaining dataset was ranked so that the most representative test for each unique interval was identified. Time constraints for the current project precluded the evaluation of the post-Montney pressure data.

A number of Dominion Land Survey Legal Subdivisions (LSD) and National Topographic System Units recorded more than one Upper or Middle Montney well event with QC'd data. In order to facilitate the interpretation, the dataset used in the Pressure vs Elevation (PE) plots and Pressure Depth Ratio (PD) maps, with a few exceptions, captured a maximum of one unique value for an LSD or Unit. The data count as distributed amongst the formations considered for this section:

Summary of Quality Screened Data

Stratigraphic Interval	DSTs	AB AOFs	BC AOFs	OZPs	Total Tests Passing QC	Mapped/Plotted Tests
Debolt	17	0	7	0	24	24
Stoddart	41	34	31	0	106	106
Belloy	111	3	57	3	174	174
Lower Montney	0	0	0	0	0	0
Middle Montney	9	24	177	5	260	215
Upper Montney	2	7	516	0	791	525
Commingled Montney	0	0	7	0	7	7

Table 4. QC Pressure data distribution by stratigraphy and test class. Some tests were redundant for mapping purposes.

Interpretation

Upper Montney

The PD mapping of the Upper Montney outlined several transitions across the study area from relatively high (> 14 kPa/m) to low (< 10 kPa/m) PD values (see Figure 13). Notwithstanding the uncertainty inherent in fault placement, a relationship between fault patterns and these hydrodynamic discontinuities is evident. As noted earlier, these discontinuities are likely caused by faulting within or beyond the level identifiable by conventional means such as seismic. Distinct variations in pressure gradient could be used as a method to identify strike-slip and other faults that are otherwise difficult to discern in seismic or other data. Some of the discontinuities in Figure 11, appear to have a relationship to the NRCan seismic events outlined in Figure 12. However, additional work establishing the spatial and temporal relationship between the NRCan seismic events, inferred faults, hydrodynamic discontinuities, completion formation intervals and oil and gas activities is required to further understand this potential correlation. Figure 14 outlines the faults from Figure 11 that appear to be hydraulically conductive or non-conductive (referred to as Hydrodynamic Discontinuities) overlain on the Upper Montney PD Map. The presence of some possible additional discontinuities has been inferred based on the pressure trends. This implies a relationship in which certain faults have increased the system permeability and allowed pressure leakage while other faults have not increased the system permeability and, thereby, preserved higher relative pressure.

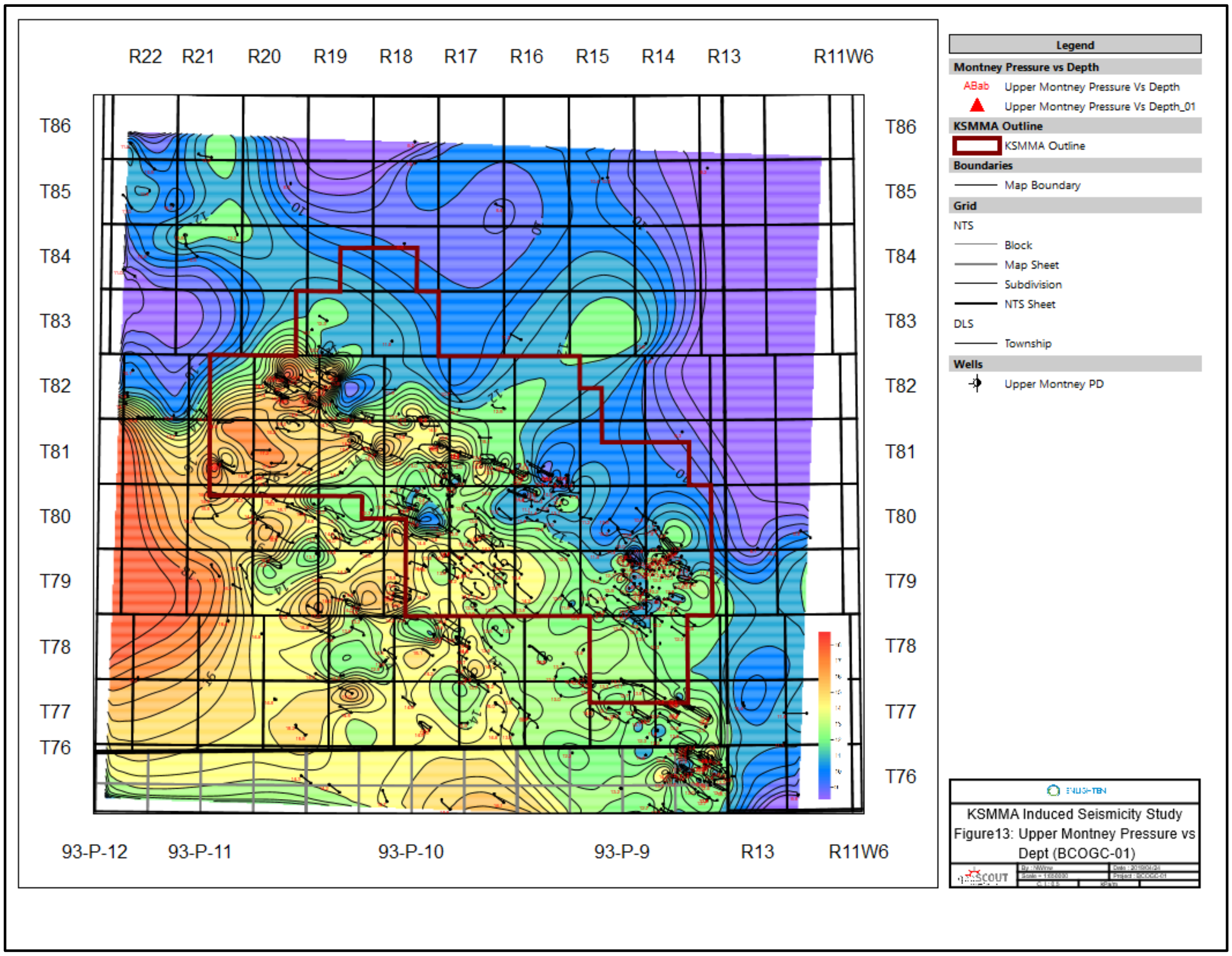

Figure 13. Upper Montney pressure vs depth ratio map.

It is important to stress that although these faults appear to have allowed for discrete and localized pressure depletion at the Montney level, as with the discussion about faulting, there is no implied pathway to allow the transmission of gas and/or completion fluids to surface. A significant number of factors militate against this manner of vertical migration. These factors include:

- Presence of Doig Phosphate interval as a primary top seal to the Montney
- Significant number of sealing formations above the primary seal
- En echelon nature of faults as described earlier
- Buoyancy effects promoting lateral migration within overlying formations

The Hydrodynamic Discontinuities were incorporated into the data gridding to conceptually highlight the distribution of pressure terranes. This refines the PD trends (Figure 15) and helps identify potential Pressure Terranes (Figure 16). Additional work is needed to confirm and further refine these features.

The UM PE plot (Figure 17) illustrates the pressure data distribution. Since the pressures within each Terrane can vary over a large elevation range the assignment of pressure gradients was impractical.

Each Montney datapoint has been assigned to a Terrane based on its geographical location. These data have been posted to the data points on the PE plot (Figure 17).

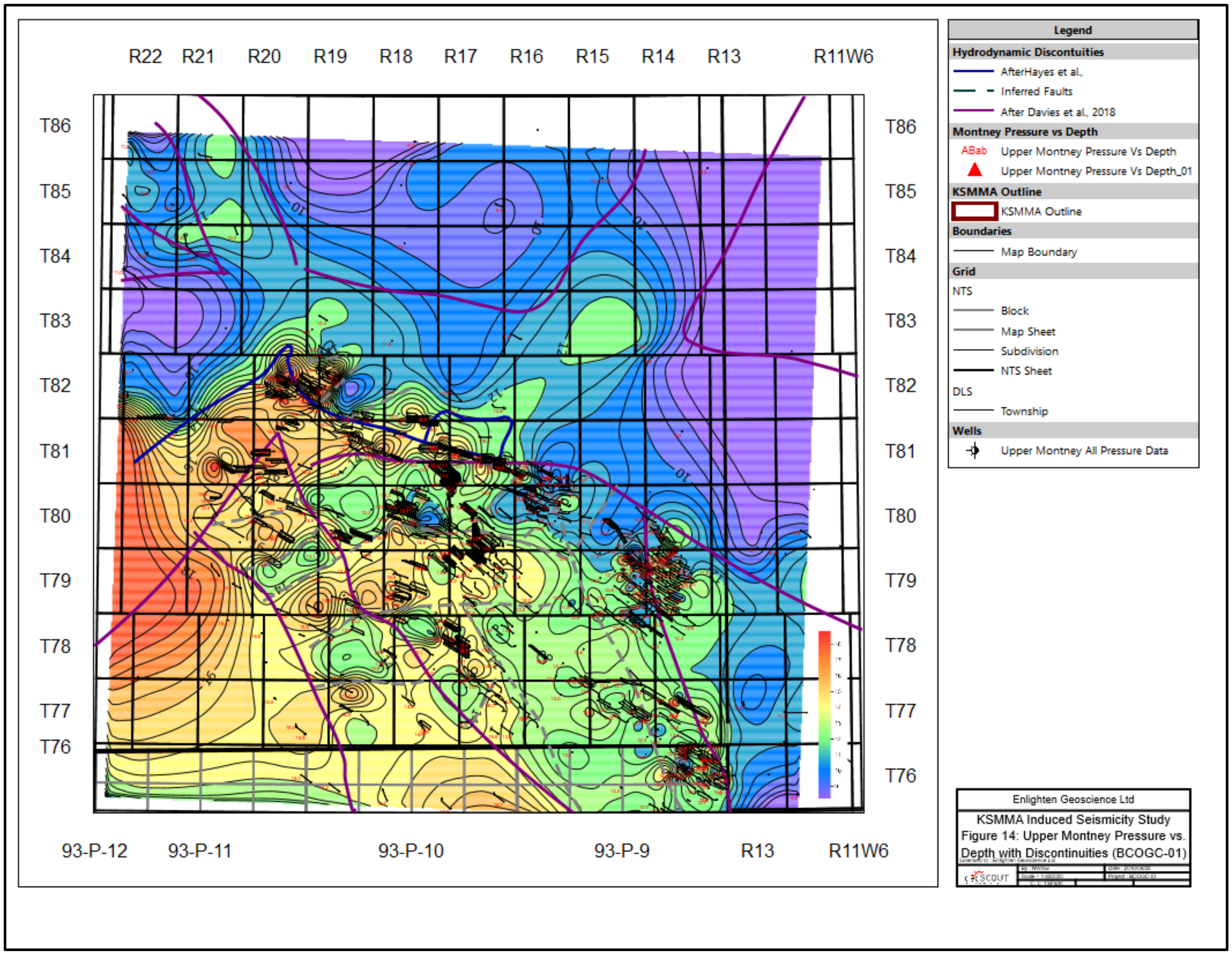

Figure 14. Map of Upper Montney pressure vs depth overlain with Hydrodynamic Discontinuities.

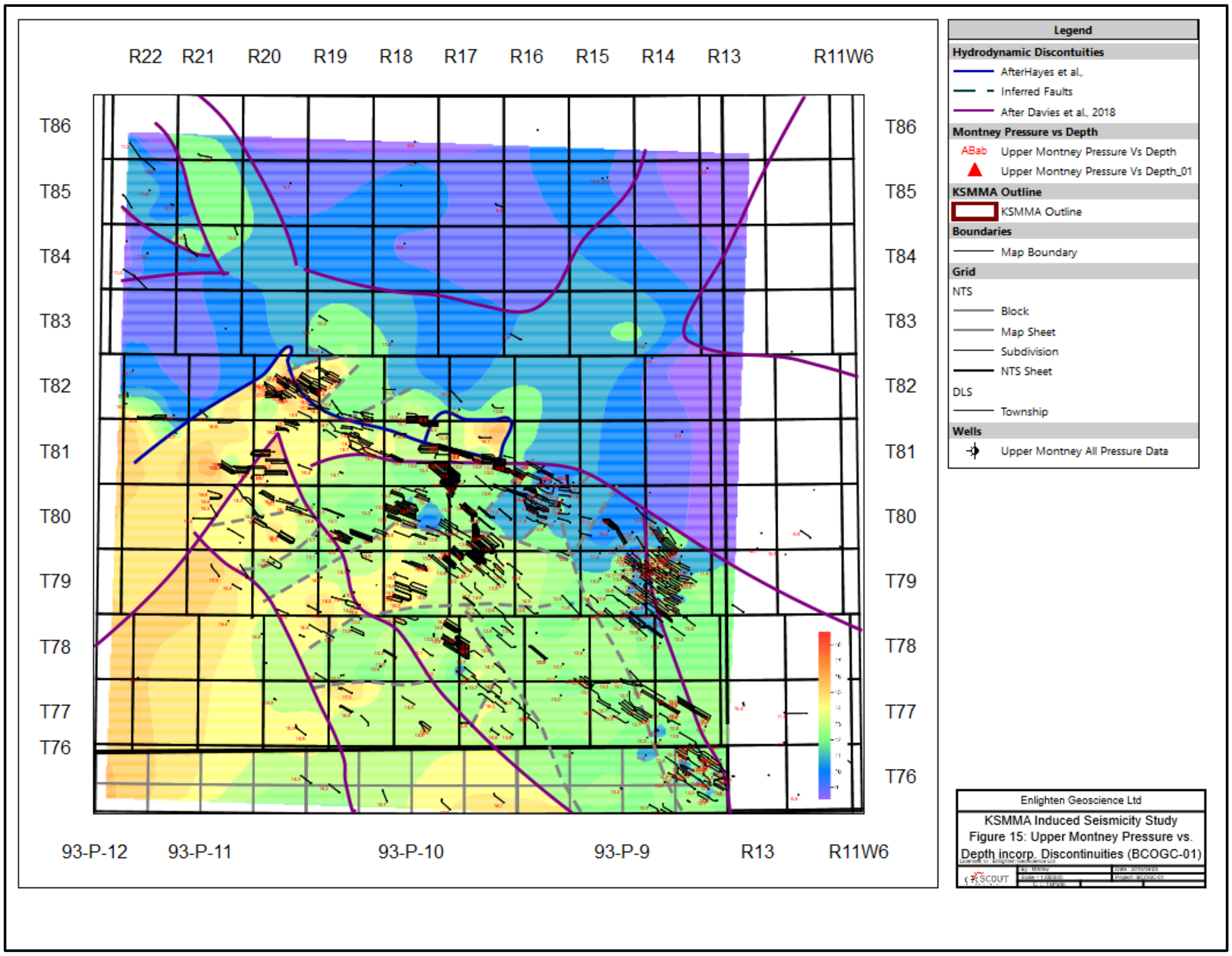

Figure 15. Upper Montney pressure vs depth recontoured to incorporate Hydrodynamic Discontinuities.

© 2019 Enlighten Geoscience Ltd.

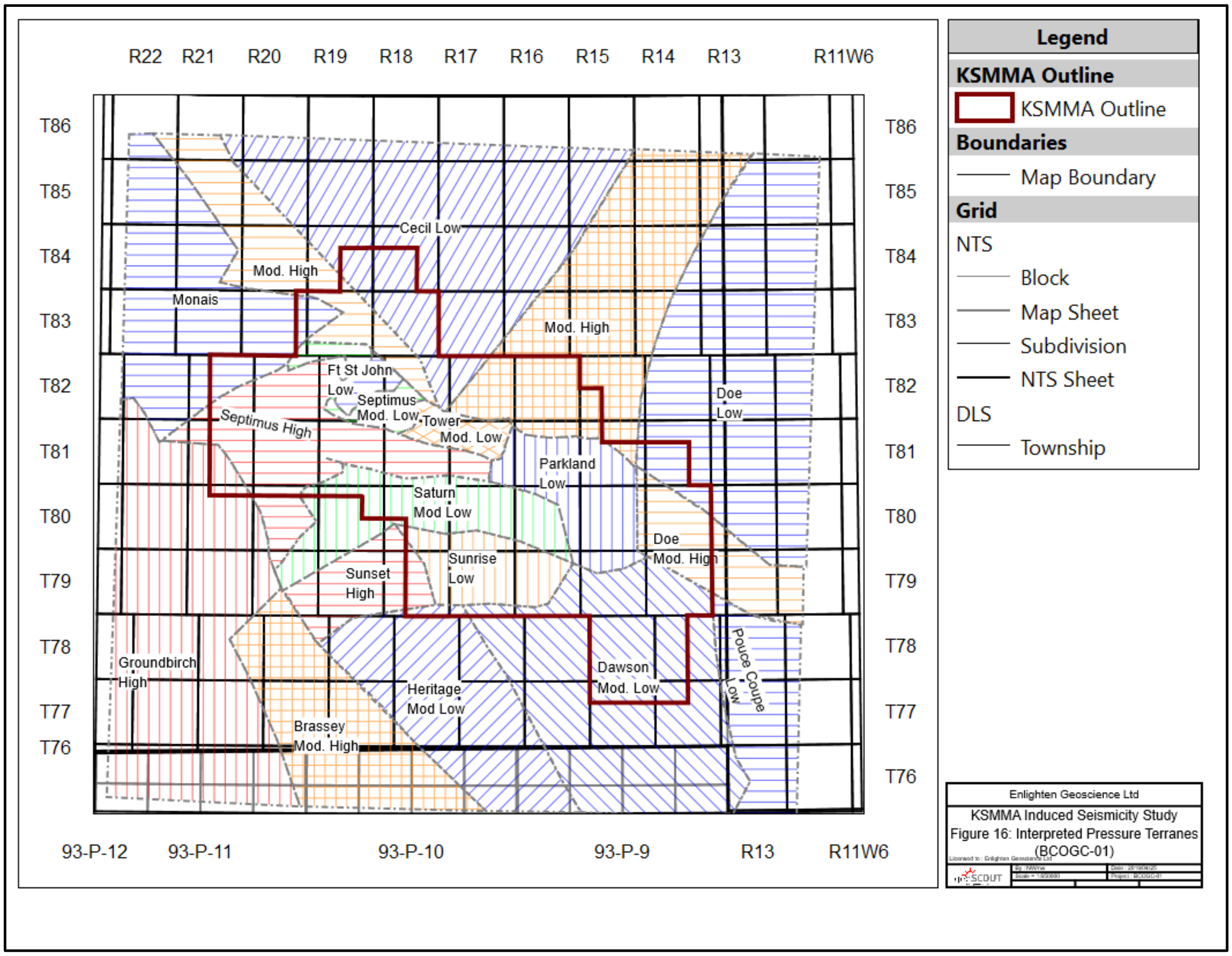

Figure 16. Interpretation of Montney Pressure Terranes. Used to display first-order concept of Hydrodynamic Discontinuities.

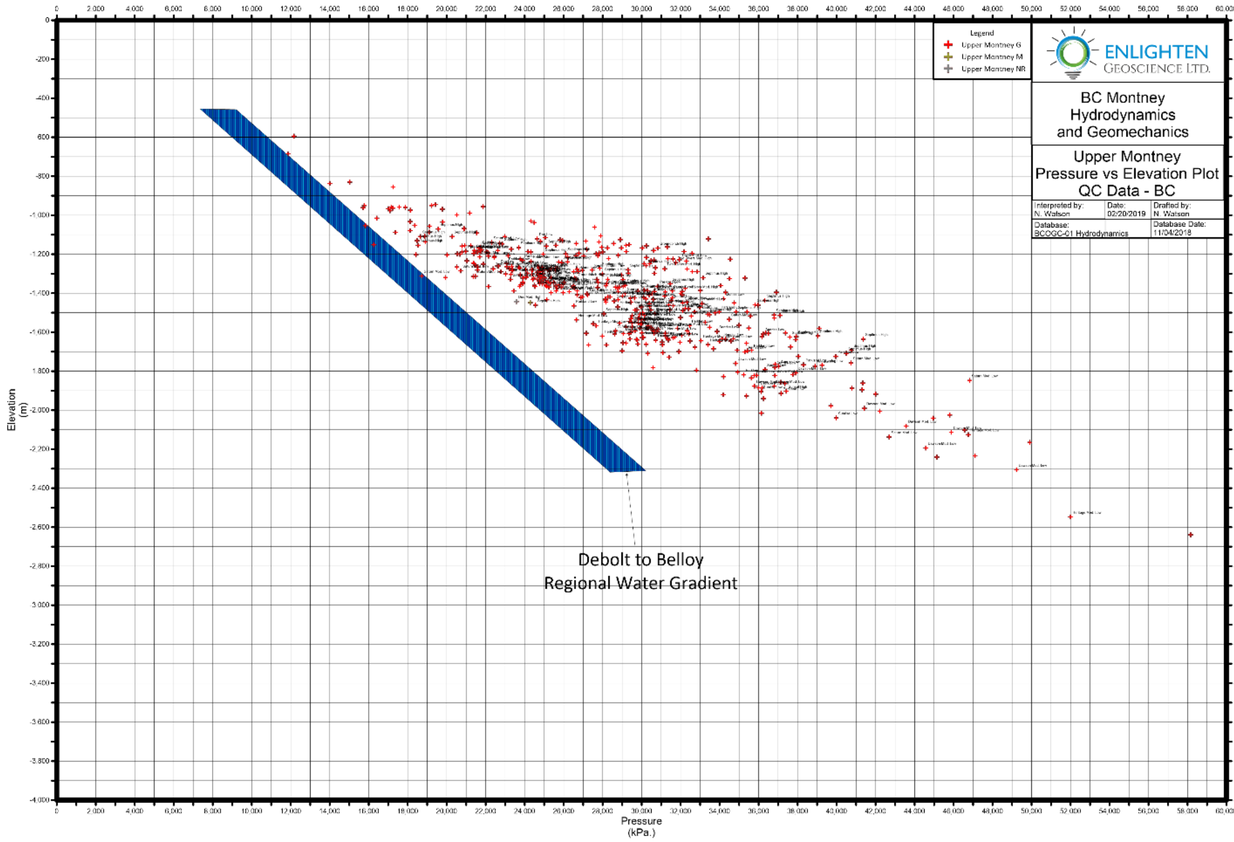

Figure 17. Upper Montney pressure vs elevation plot.

Middle Montney

The Middle Montney has a little over half of the number of QC pressure tests available for mapping (Figure 18). In a similar fashion to the Upper Montney, regridding the Middle Montney PD data relative to the Hydrodynamic Discontinuities establishes preliminary pressure terranes (Figure 19).

The relationship of the Middle Montney pressures to the Regional Debolt to Belloy water gradient is shown in Figure 20.

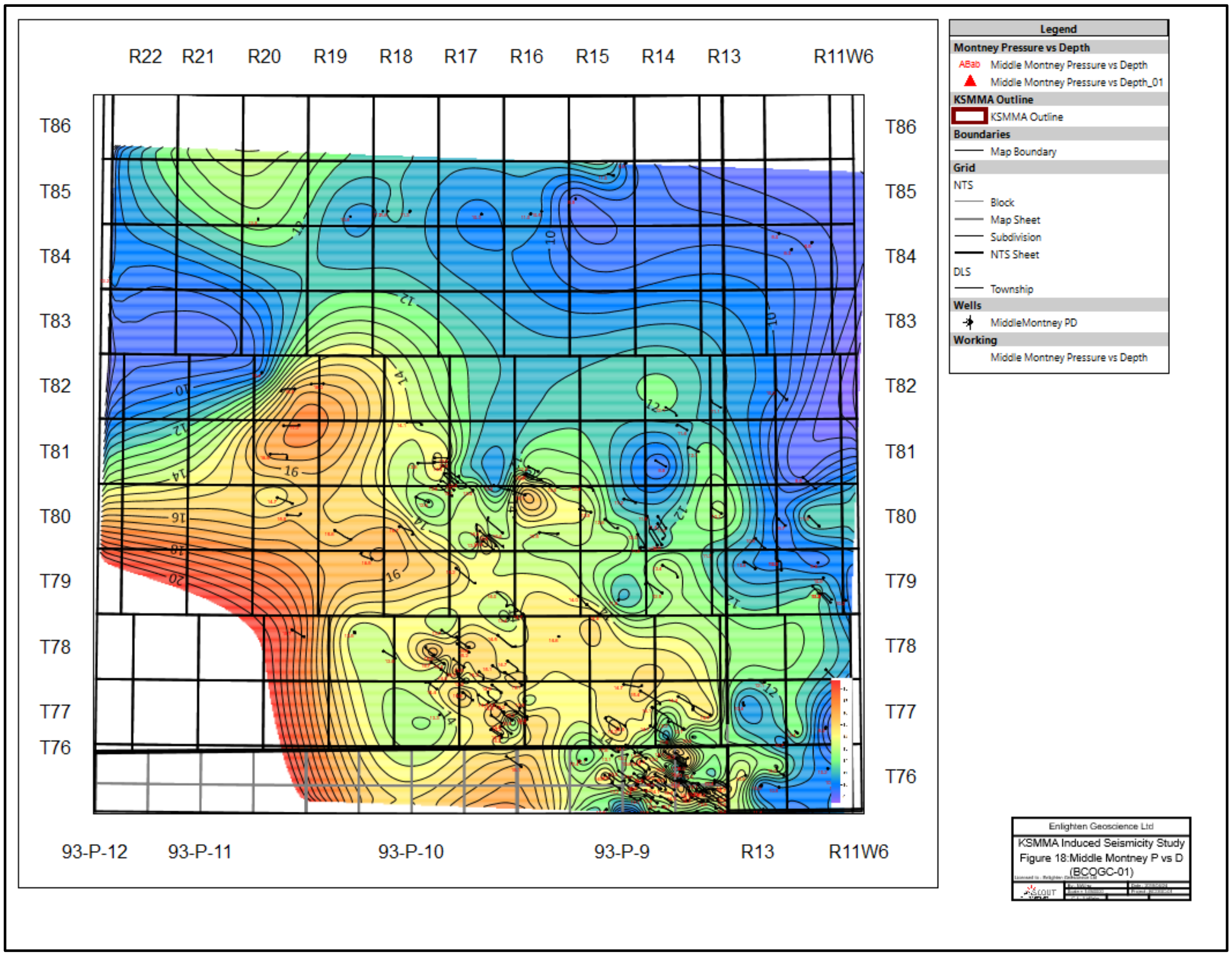

Figure 18. Middle Montney pressure vs depth ratio map.

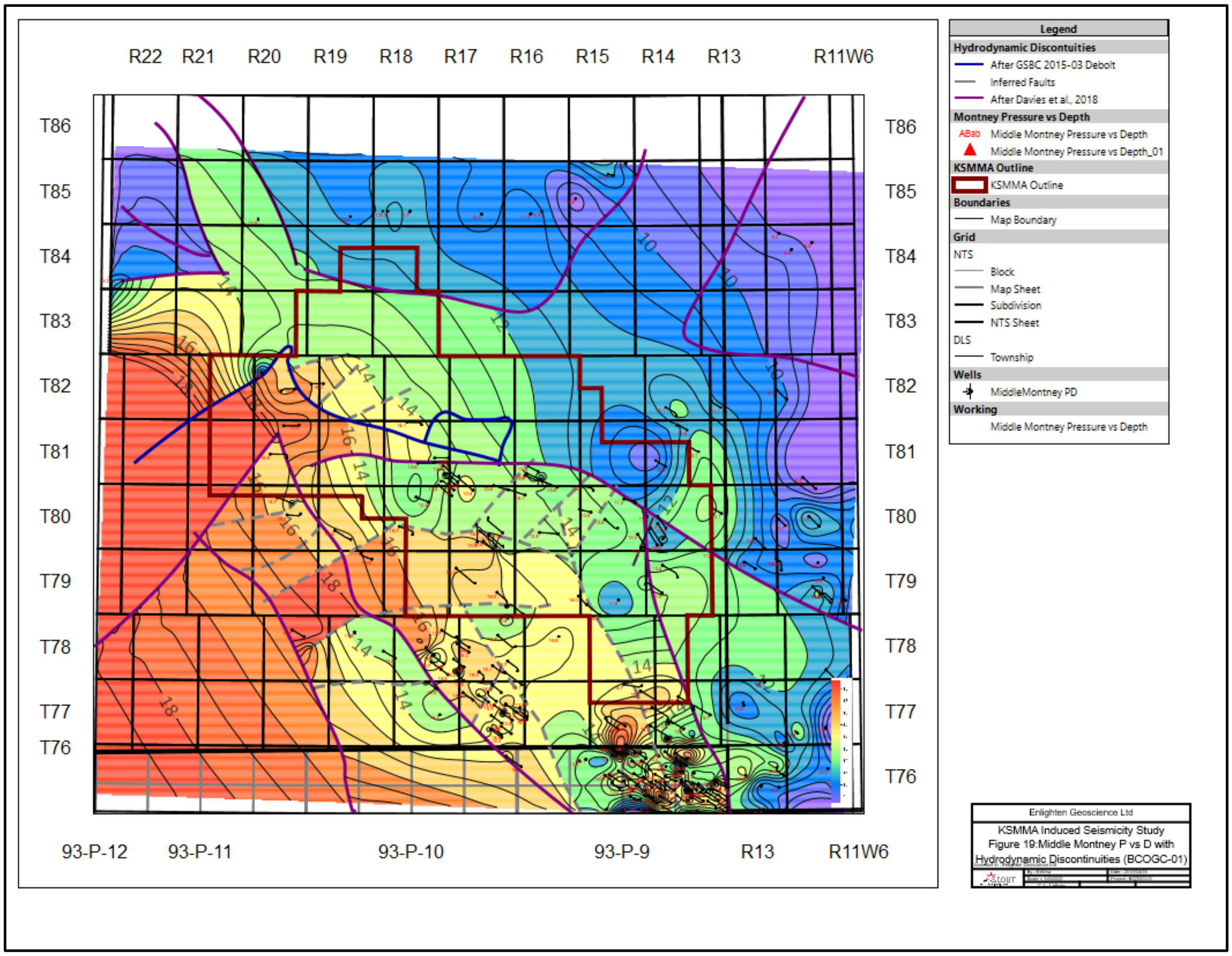

Figure 19. Middle Montney pressure vs depth incorporating Hydrodynamic Discontinuities.

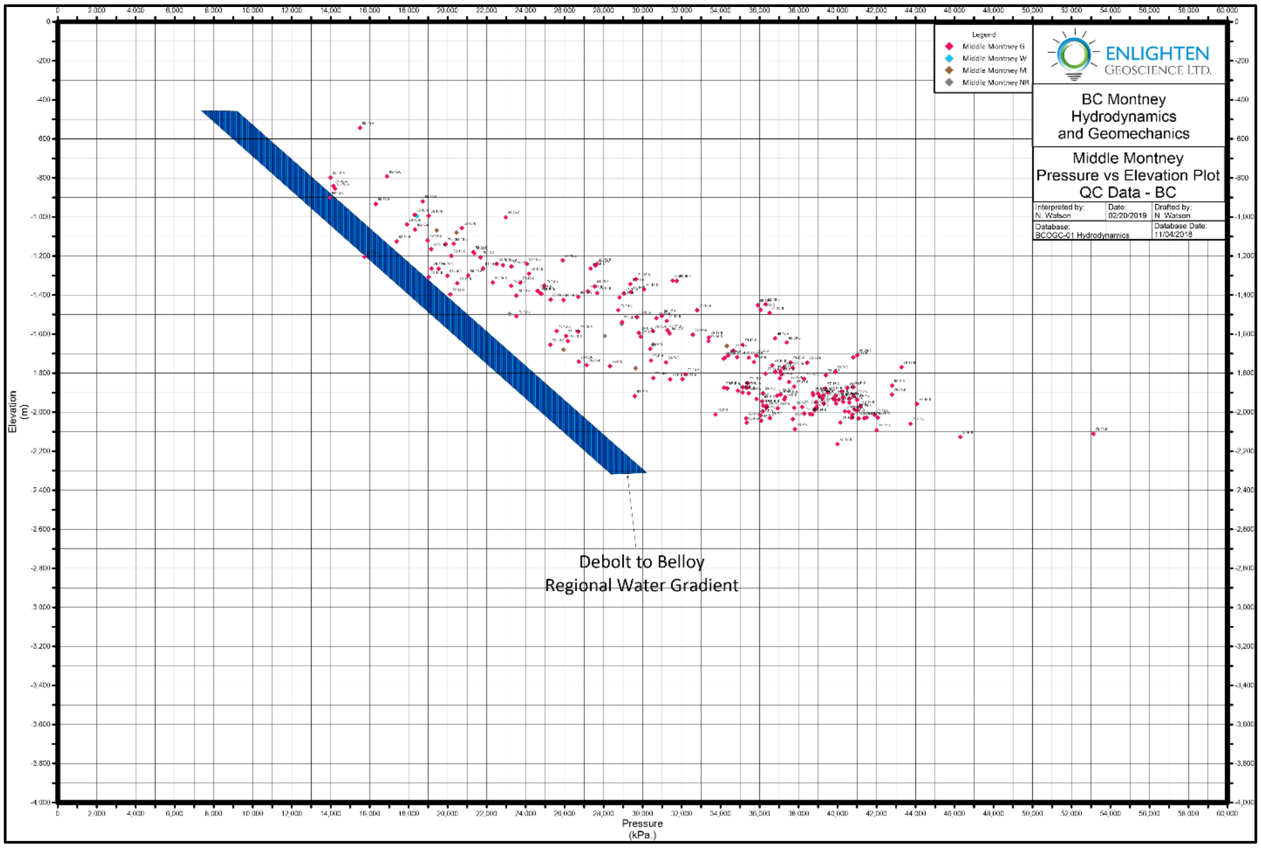

Figure 20. Middle Montney pressure vs elevation plot.

Underburden (Debolt to Belloy)

These formations demonstrated a mix of hydrocarbon and formation water consistent with the expectation that the underburden is within a deep, saline aquifer setting. Fifteen tests recorded pressure vs depth ratios greater than 11.5 kPa/m, placing them in the category of being over-pressured. Given the regional setting, the offsetting pressures at hydrostatic levels and the co-production of formation water, these formations are not considered to be within a Higher Pressure Deep Basin (HPDB). The most likely reason for the over-pressuring would appear to be significant relative uplift. The distribution of these pressures relative to test elevation is shown in Figure 21.

The Debolt to Belloy pressure vs depth ratio map is shown in Figure 22. Although the contours align with the fault maps somewhat, the correspondence with the pressure compartments is variable (i.e. good match with the Sunset High, reasonable with Heritage Low and Two Rivers High, poor with other compartments) suggesting that the pressure preservation is likely controlled by other fault sets.

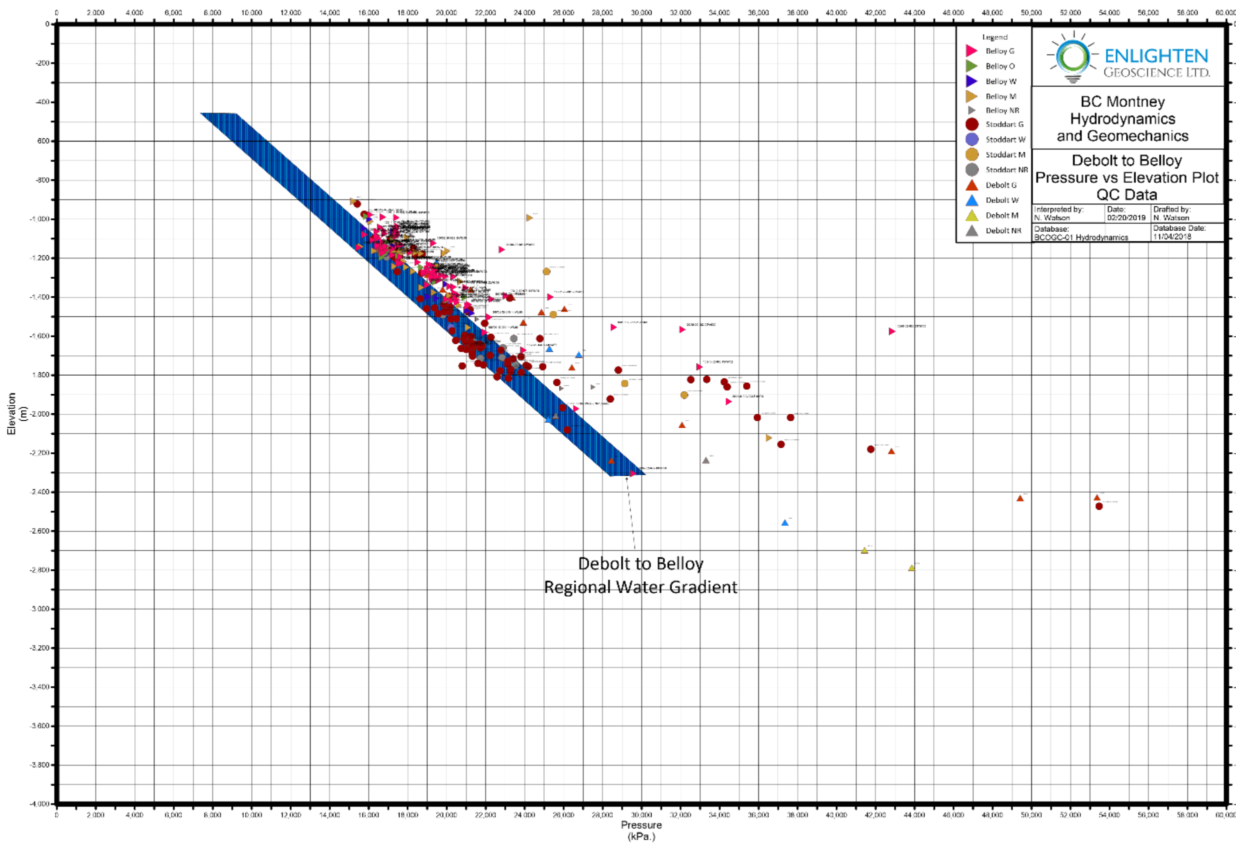

Figure 21. Debolt to Belloy pressure vs elevation graph.

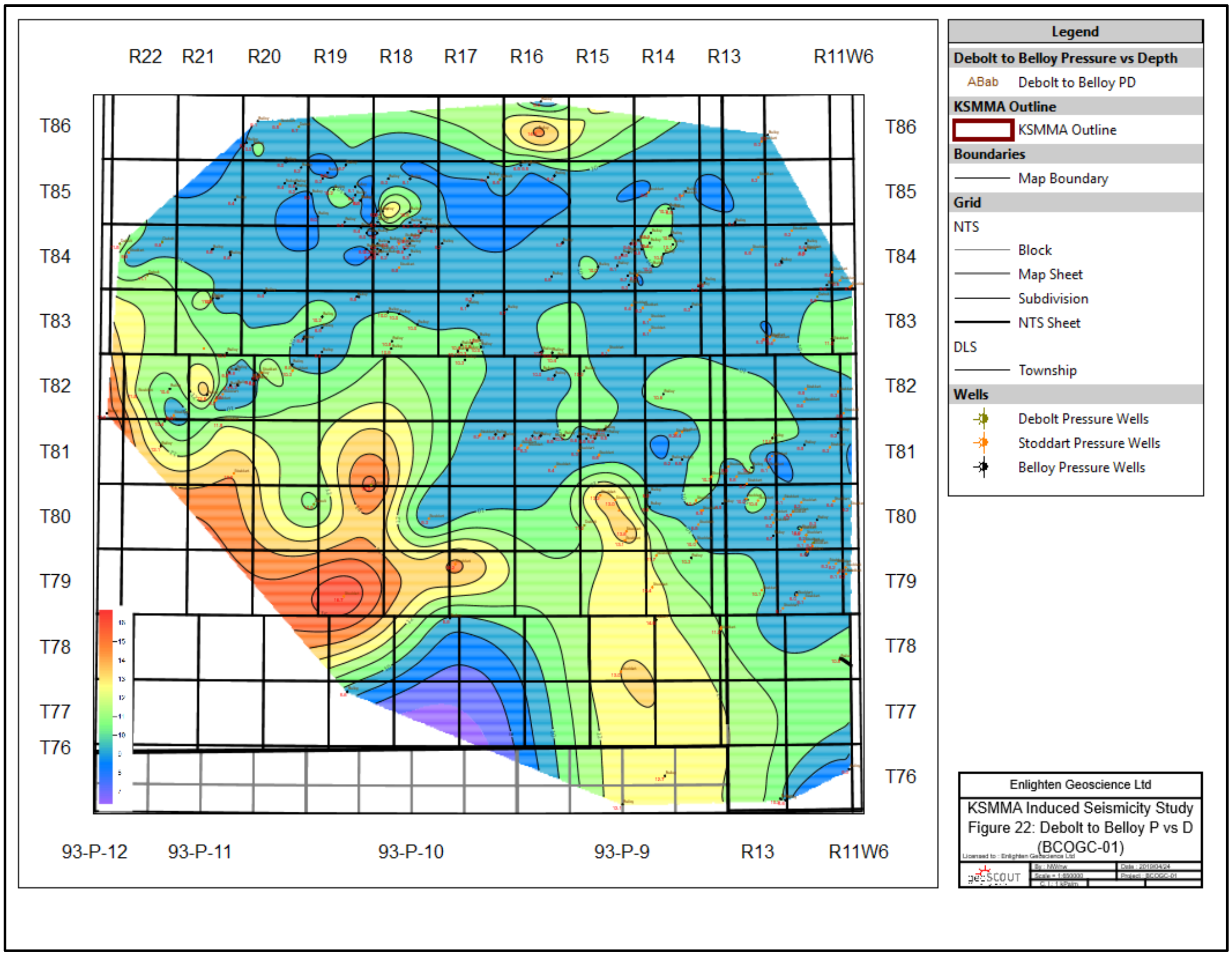

Figure 22. Debolt to Belloy pressure vs depth map.

VI. Geomechanics

While there exist several published compilations of regional stress that include the KSMMA area (e.g., Grasby et al., 2012), a much more detailed understanding is needed within the study area in order to potentially relate induced seismicity risk to variations in stress or other, related factors. In this study we determine the full state of in situ stress in several locations throughout the study area. We then looked at the implications the stresses have for the frictional stability of fractures and faults.

In Situ Stress Determination

The state of stress is described by three principal, orthogonal stresses, each with a unique magnitude and orientation. In most cases one stress is vertical (the overburden) and two are horizontal. The magnitude of the vertical stress is easily determined using density log data or average densities for the overlying formations. The magnitude and orientation (vertical or horizontal) of the minimum stress is determined primarily from minifrac test results. The maximum horizontal stress is determined by finding a value that would cause stress-induced borehole failure (or lack thereof) that matches observed failure in image log data or failure indicated by caliper enlargements and/or drilling events. The orientation of the observed failure provides the azimuth of S_{Hmax}. A much more detailed discussion of stress determination may be found in Zoback (2010).

Stress-induced Borehole Failure

The best data for identifying stress-induced failure (breakouts and tensile cracks) are borehole image logs such as Schlumberger's Formation MicroImager (FMI, an electrical image log) or Baker Hughes' Circumferential Borehole Image Log (CBIL, an acoustic image log). Unfortunately, because of their large file sizes and challenges in reproducing them, image logs are relatively difficult to find in the public databases. Even when they are found, image quality can often be so poor as to preclude any kind of analysis.

For this study, 17 image logs were found in the public data: 6 images were of high enough quality for interpretation, 6 were of fair quality (partly or somewhat interpretable), and 5 were uninterpretable. For one of the wells with an uninterpretable image, a KSMMA operator provided a higher quality version, and the image is therefore considered proprietary. The operators provided an additional 7 image logs that were unavailable in the public data.

The timeline and scope of the current project did not allow for a detailed analysis of all the image logs. In total, 5 operator images and 3 public images were analyzed for wellbore failure in the Doig, Montney and/or Belloy. Examples of identified features are shown in Figure 23.

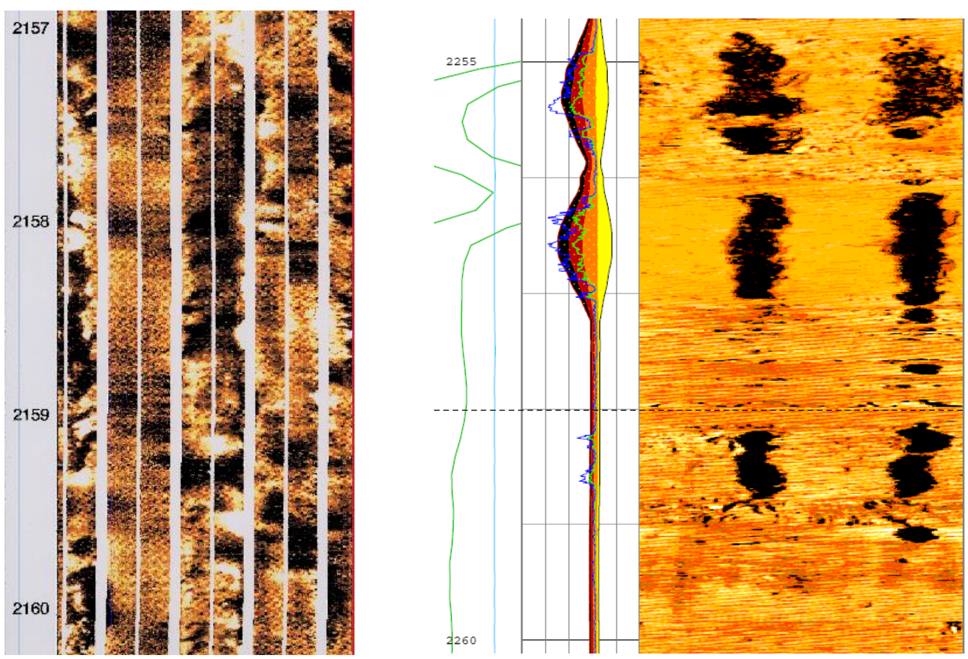

(a) (b)

Figure 23. a) Breakouts in the Doig seen in an electrical (FMI) image from well 100/01-03-081-21W6/00, b) breakouts in the Belloy seen in an acoustic (UBI) image from well 102/13-07-080-14W6/00.

Rock Strength

Unconfined compressive rock strength (UCS) is critical for using compressive borehole failure (breakouts) to determine S_{Hmax}. The KSMMA operators provided data from a total of 7 triaxial test suites that were not found in the public databases. Data from 10 additional wells were found in the BC OGC well files, and data for 6 wells were found in the AER databases. Triaxial testing programs are most often designed to obtain static and dynamic rock modulus values (e.g., Poisson's ratio), not necessarily to obtain rock strength properties, and therefore usually only about half or less of all test suites are typically useful for determining UCS. In this case 11 wells had data suitable for determining UCS – 10 in the Montney and 1 in the Doig. These data were used to determine the most appropriate equations for calculating UCS from logs (e.g., Khaksar, 2009), which is needed to determine UCS in the zones where borehole failure is observed.

Vertical Stress

The magnitude of the vertical stress was calculated at the middle of the Montney using public density logs from 12 wells across the study area. Although this is only about 1 well per 10 townships, the resulting stress value was very consistent across the area with an average of 25.1 kPa/m. Since density logs are relatively easy to obtain, a more detailed map, or maps in other zones, could be constructed fairly easily, but it is not expected that significant variation will be found, or that any variation will add to the understanding of induced seismicity in the area.

Minimum Horizontal Stress

As discussed regarding the mini-frac data in Section II, the minimum horizontal stress (S_{hmin}) in the study area is less than the vertical stress. Appendix B discusses in detail the challenges inherent in interpreting minifrac tests for S_{hmin}. For the purpose of the S_{Hmax} modeling, we derived our own best estimate for S_{hmin} from public minifrac tests located as close as possible to each of the modeled wells.

Maximum Horizontal Stress Orientation and Magnitude

Figure 24 presents data from the World Stress Map (Heidbach et al., 2018; Heidbach et al., 2016). The long axis of the map symbols represents the orientation of the maximum horizontal stress, and the middle portion of the symbols indicates what type of data were used to determine it. If a symbol is coloured, then the relative stress magnitudes were determined. Data are clearly very sparse in the greater KSMMA. There are only two data points with relative stress magnitudes on the map, one from east of the study area and one to the south, and both indicate thrust-faulting environments where the minimum principal stress is vertical. These two data points are both from earthquake focal mechanisms located at depths greater than 5,000 m.

Detailed mapping of maximum horizontal stress azimuth was not possible within the scope of this study, but general observations were made. In most wells the overall stress orientation agrees with the nearly 45° northeast-southwest trend seen on the map, although some significant rotations were observed. It is not possible at this point to comment on whether there are any kind of systematic changes in S_{Hmax} orientation across the study area or with depth. A detailed study of stress orientation would include using all available well data types including borehole failure in image logs, oriented caliper logs and azimuthal shear to determine S_{Hmax} azimuth in as many wells as possible and in individual formations or sub-units. Microseismic data and dense array seismic monitoring data may also provide valuable information.

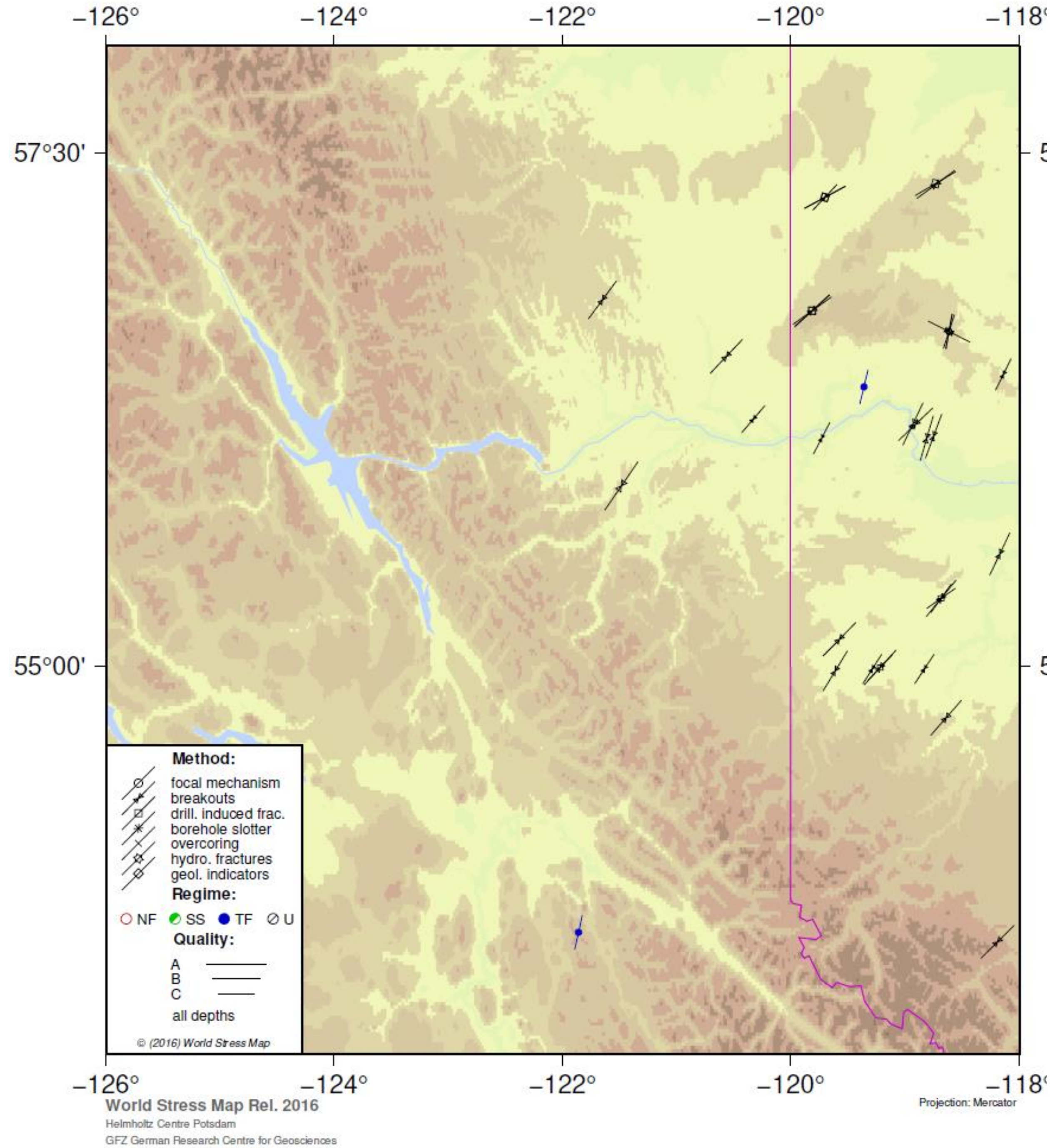

Figure 24. World Stress Map data for the region surrounding the study area.

S_{Hmax} magnitude was determined in each of the 8 wells in which wellbore failure was identified. Modeling for S_{Hmax} magnitude was primarily based on compressive wellbore failure (breakouts), although tensile failure (cracks) was also observed in some of the wells. The results in all 8 wells (Figure 25) indicate that at the depth of the Doig through Belloy, the current-day state of in situ stress can be categorized as strike-slip (Anderson, 1951), where the vertical stress is intermediate between the minimum and maximum horizontal stresses. This is consistent with the presence of tensile failure in some of the wells. It is in contrast, however, with the two deeper focal mechanism points on the World Stress Map (Figure 24) which indicate thrust faulting at basement depths. Moment tensor solutions for the November 2018 induced events indicate largely reverse-faulting motion with some strike-slip component. Fault motion is not a direct indicator of principal stresses particularly when slip is on pre-existing faults. At present, the resolution at which in situ stress has been determined in the KSMMA is not adequate to address the implications of the induced event moment tensors. Microseismic interpretation could be a very important contribution towards a better understanding. Microseismic data are all proprietary and were not shared with Enlighten for this study.

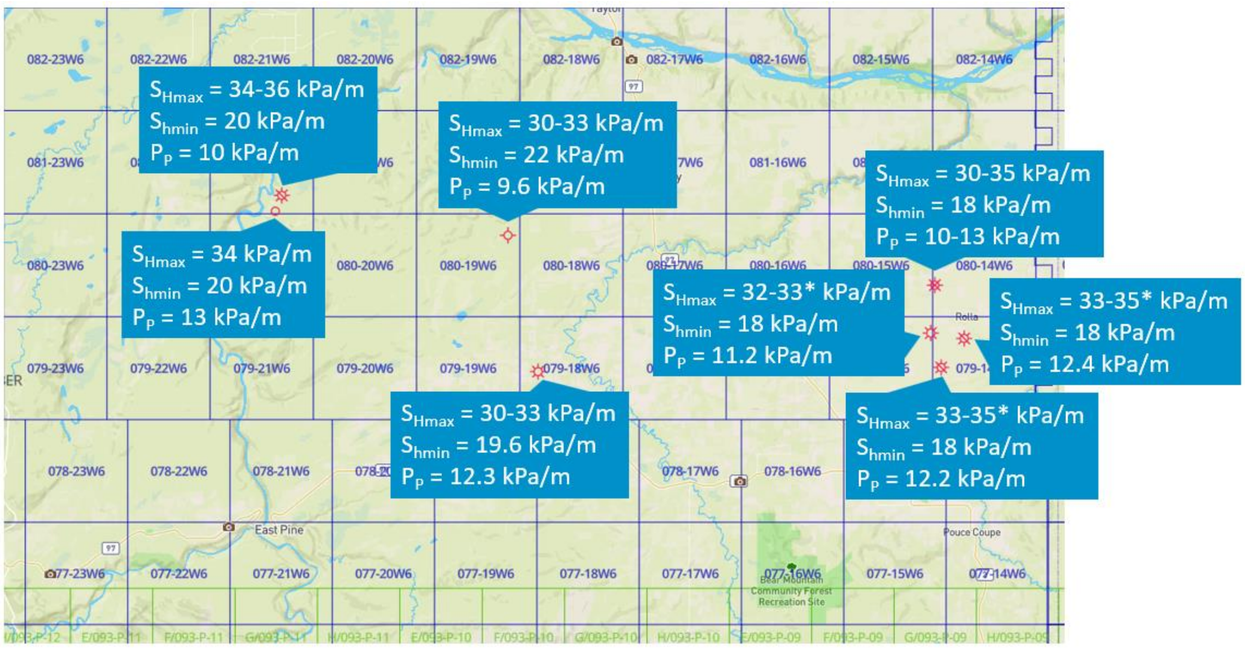

Figure 25. Pore pressure (P_P), minimum horizontal stress (S_{hmin}) and maximum horizontal stress (S_{Hmax}) magnitudes determined in the study. An asterisk (*) indicates added uncertainty because mud weight information had to be obtained from log headers instead of daily drilling reports.

Critically Stressed Fracture Analysis

Natural Fracture and Fault Populations in the Study Area

Generally, our only understanding of the existence of natural fractures or faults in the subsurface at sub-seismic scales comes from image logs and core. Of the 17 image logs found in the public data sets for this study, 8 had interpretations for natural fractures. In one additional case an interpretation was found, but the image itself was not. Of the 8 image logs provided by the operators, 6 had interpretations for natural fractures. In one additional case, an operator provided an interpretation for an image log that was found in the public data.

The fracture interpretations are from wells across the study area. While most cover the Montney, some of the public ones cover intervals above or below the Montney. The interpretations were performed by a variety of companies including Weatherford, Baker Hughes, Schlumberger, Precision and HEF Petrophysical. Interpretation methods and results will vary between the different companies, making it difficult to compare the interpretations. Regardless, a map summarizing the public interpretations is provided in Figure 26. In general, fractures and structures are seen above and below Montney, but very few features are picked in the Montney itself except for one well quite far to the south. The Belloy is in some cases heavily fractured, raising the question of whether it is providing fluid communication to faults under the Montney in the KSMMA.

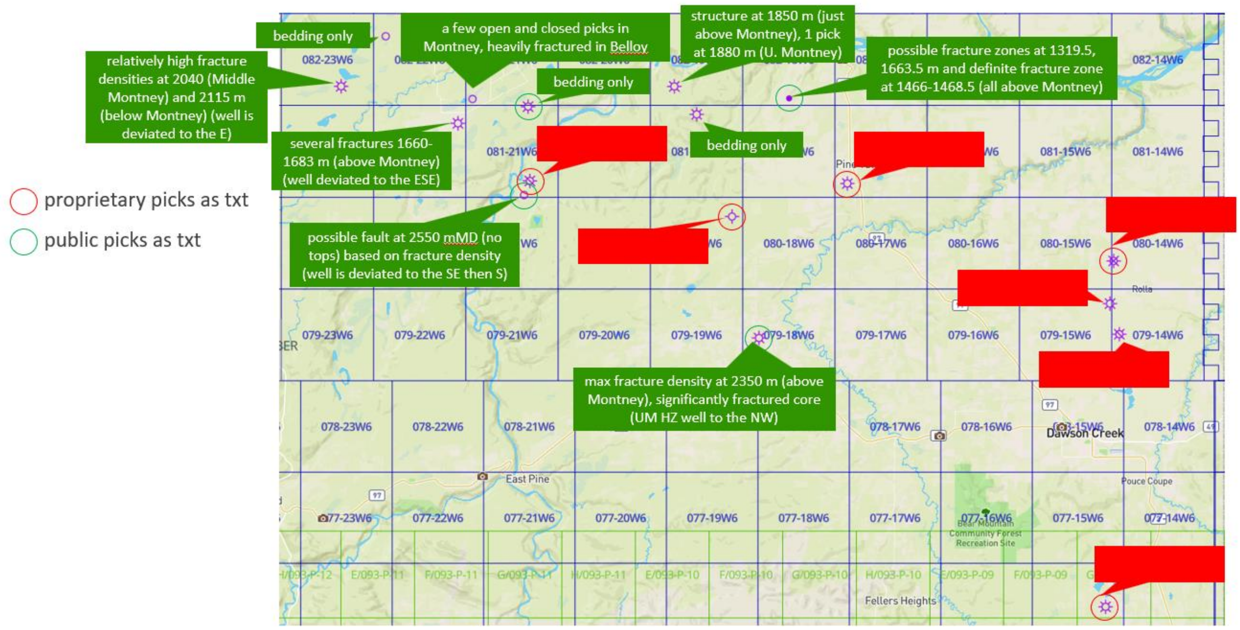

Figure 26. Map and summary of natural fracture interpretations from image logs. Red boxes indicate proprietary interpretations.

In addition to the image log analyses, two fracture studies were found in the OGC well files. One is a thin section study of the Doig (Jamison, 2011), and the second is a core study of the Montney (Gillen, 2017). The Doig study included data from multiple wells and reported two predominant deformation types: wavy/undulating extensional fractures at high angles to bedding, and shear fractures/zones sub-parallel to bedding, some with strongly slickenslided surfaces. Many of the observed features show evidence of multiple crack-seal episodes, and some of the shear features contain granulated fracture filling or bits of broken off host rock. The Montney core study identified many “horizontal break” features, especially in the lower section of the core, some contain microjointing and/or slickenslides. Most of the fractures observed were calcite-filled. There was one significant unmineralized fracture that was very planar and cut completely through the core (sampled length of 41 cm). It was found that steep to vertical, calcite filled fractures correlate to gamma lows and faults correspond to gamma highs, suggesting a relationship between mineralogy and fracturing style.

In the search for mechanical core tests, 32 wells were found to have white light photos of core (whole or slabbed) in the OGC well files. Six sets of photos were reviewed as part of the study because they were in wells that also had image logs. Upon this cursory review it appears that several of the cores contain significant natural fractures, although these can't yet be assigned to specific stratigraphic intervals. Several additional sets of photos are available in Alberta just east of the KSMMA. The cores obviously represent another important data source for natural fracture characterization. No evidence of core-based fracture analyses other than the reports discussed in the previous paragraph was found during the study.

Critically Stressed Fracture/Fault Analysis

Most cases of induced seismicity can be explained by Mohr-Coulomb theory (Ellsworth et al., 2018). For any fracture or fault, the normal stress acting perpendicular to the fracture/fault and the shear stress acting along the fracture/fault plane can be calculated from the three-dimensional state of in situ stress and the fracture/fault's orientation. Mohr-Coulomb theory says that fractures/faults with a high amount of shear stress relative to effective normal stress (total normal stress minus the pore pressure) are frictionally less stable than those with a lower ratio of shear to effective normal stress. The risk of slip is also dependent on the frictional properties (cohesion and coefficient of sliding friction) of the fracture/fault plane.

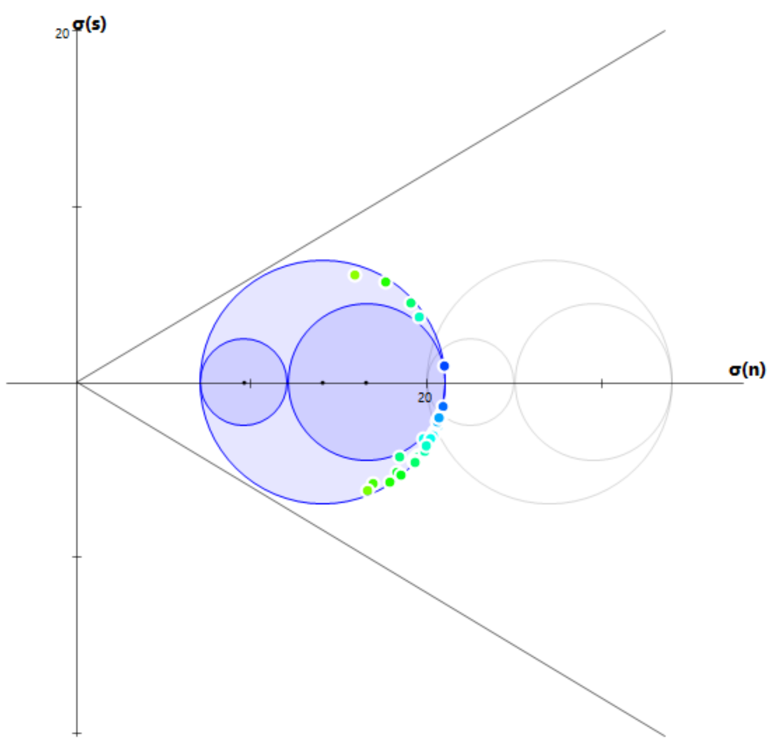

Figure 27. Mohr diagram for fractures identified in well 100/01-03-081-21W6/00. Inputs: S_{hmin} = 40 MPa, S_V = 50 MPa, S_{Hmax} = 68 MPa, P_P = 26 MPa.

Figure 27 is a Mohr diagram for fractures identified in well 100/01-03-081-21W6/00. It was constructed using stresses determined from modeling wellbore failure in the same well. Effective normal stress (= normal stress – pore pressure) is plotted on the horizontal axis, and shear stress is plotted on the vertical axis. The larger circle encompasses the possible shear vs effective normal stress values for fractures/faults of all possible orientations in the given stress state. The coloured points represent

© 2019 Enlighten Geoscience Ltd.

individual identified fractures and are coloured by slip risk from red (higher risk) to blue (lower risk). The straight, diagonal line represents the frictional strength of fractures/faults assuming a coefficient of sliding friction of 0.6 and zero cohesion. If the shear vs effective normal stress for a given fracture plots above this line, then it is considered "critically stressed" – that is, unstable in the given conditions. In this case the stress state is not quite critical (the circle doesn't touch the diagonal line), and most of the existing fractures are far from being critically stressed. This well was deviated to the southeast before turning south, so most of the fractures intersected are steeply dipping with strikes to the northwest and southeast. All the fractures were categorized as "resistive" in the image log analysis, meaning they were mineralized. This is consistent with fractures that are not critically stressed, as critically stressed fractures tend to be partially or wholly "open," or not mineralized/sealed.

Importantly, increasing fluid (pore) pressure acts to decrease the effective normal stress acting on a plane but does not affect the shear stress. This is the mechanism by which increasing fluid pressure in the subsurface can cause previously stable fractures/faults to become unstable. It is important therefore to understand how much pressure will potentially cause seismogenic faults to become critically stressed. It is also important to understand the frictional stability of smaller natural fractures, because the ones that are critically stressed, or nearly so, are most likely to provide conduits for fluid communication *to* seismogenic faults.

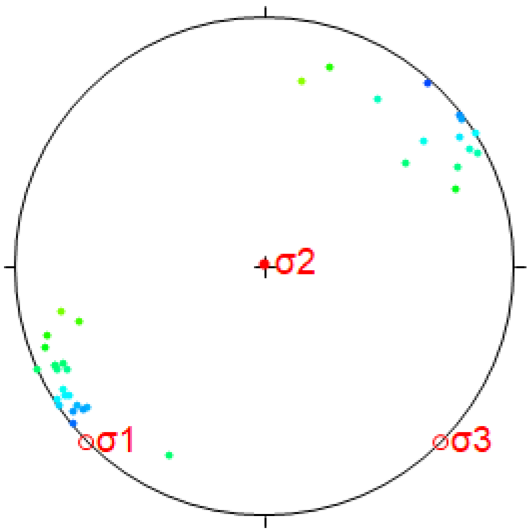

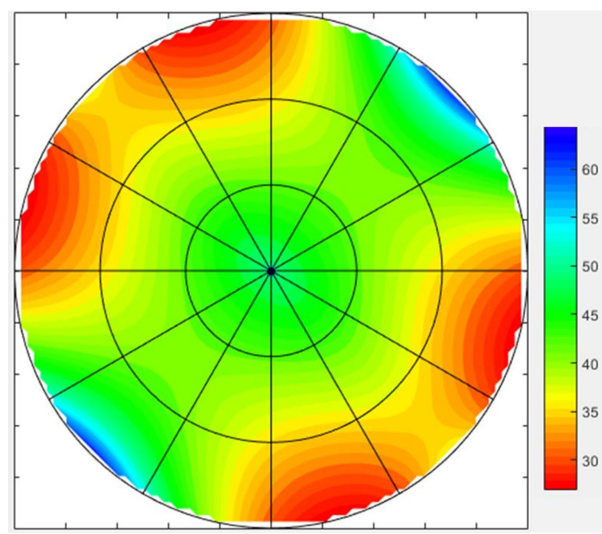

(a) (b)

Figure 28. a) Lower hemisphere stereonet of poles to fractures identified in well 100/01-03-081-21W6/00, b) Lower hemisphere stereonet for the stress state used to construct Figure 15 showing the fluid pressure (in MPa) that would cause fractures/faults of all possible orientations to become critically stressed. [Note colours in a do not directly correspond to colours in b]

Figure 28a is a lower hemisphere stereonet of poles to fracture planes in well 100/01-03-081-21W6/00; the poles are coloured by slip risk as in Figure 28. Figure 28b is a general stereonet for the same stress state showing the total fluid pressure that will cause fractures of all possible orientations to become critically stressed. It is assumed that the orientation of S_{Hmax} in this case is directly northeast-southwest. In this case, formation pore pressure is modeled at 26 MPa, so fractures will begin to become critically stressed at just a few MPa of additional pressure.

Figures 29 through 32 are Mohr diagrams and stereonets for the two other wells with public fracture interpretations available with fracture dip information in a text file. Well 102/13-17-079-18W6/00 was also a well in which stresses were modeled. For well 100/05-03-082-18W6/00, stresses from well 100/11-25-080-19W6/00 were used to construct the Mohr diagram and stereonets.

Two important points are evident from the Mohr diagrams and stereonets. First, whether there are critically stressed fractures/faults is different at the three well locations. The differences are somewhat driven by differences in stress magnitudes, but they are primarily the result of pore pressure differences, which is an illustration of how important the hydrodynamics are to the induced seismicity understanding. Second, in all cases fractures/faults that are most likely to become critically stressed due to a pressure increase strike approximately 15°-45° from the S_{Hmax} orientation and have dips greater than 60°. The USGS (2019b) moment tensor solution for the November 29, 2018 seismic event indicates primarily thrust faulting motion and nodal planes striking northwest-southeast with intermediate dips (40° and 53°). McGill University moment tensor solutions (Stu Venables, pers. comm.) for the larger events around the November 29 event indicated a combination of thrust and strike-slip motion and nodal planes striking northwest-southeast and approximately east-west. The implications of the discrepancy between the known seismic events and the most critically stressed fracture/fault orientations should be investigated further.

© 2019 Enlighten Geoscience Ltd.

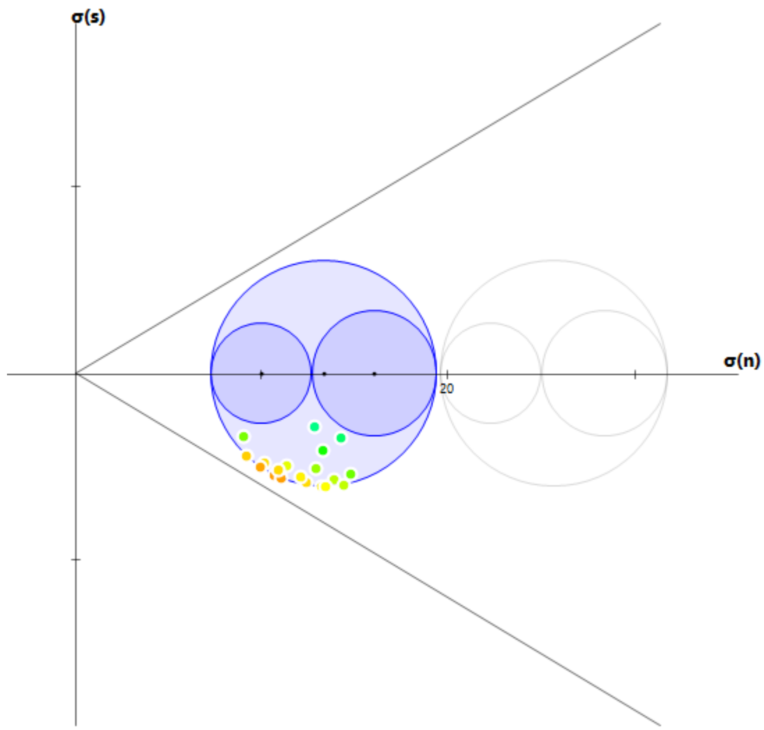

Figure 29. Mohr diagram for fractures identified in well 102/13-17-079-18W6/00. Inputs: S_{hmin} = 39.2 MPa, S_V = 50 MPa, S_{Hmax} = 63.5 MPa, P_P = 24.6 MPa.

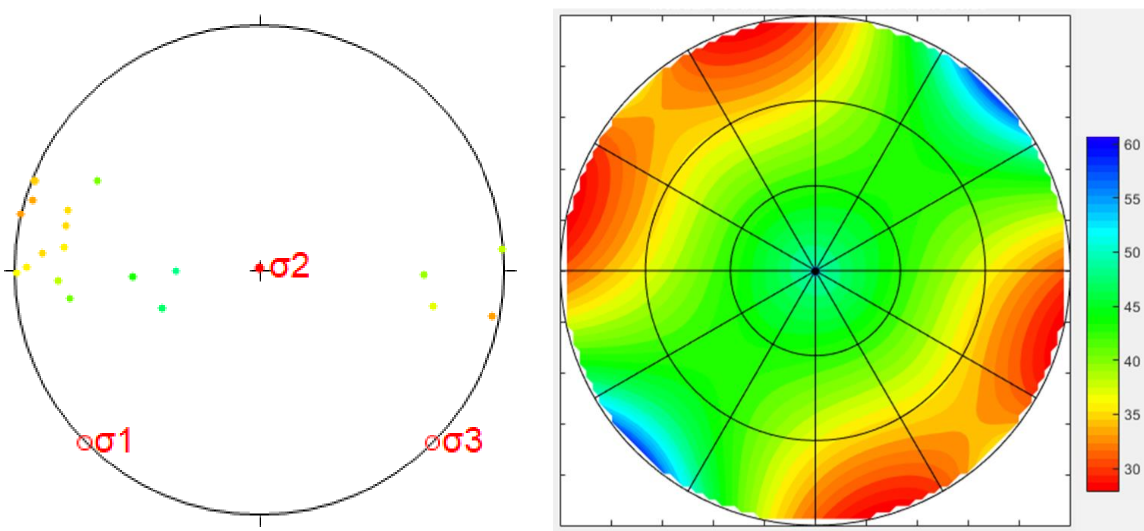

(a) (b)

Figure 30. Stereonets for well 102/13-17-079-18W6/00. [Note colours in a do not directly correspond to colours in b]

© 2019 Enlighten Geoscience Ltd.

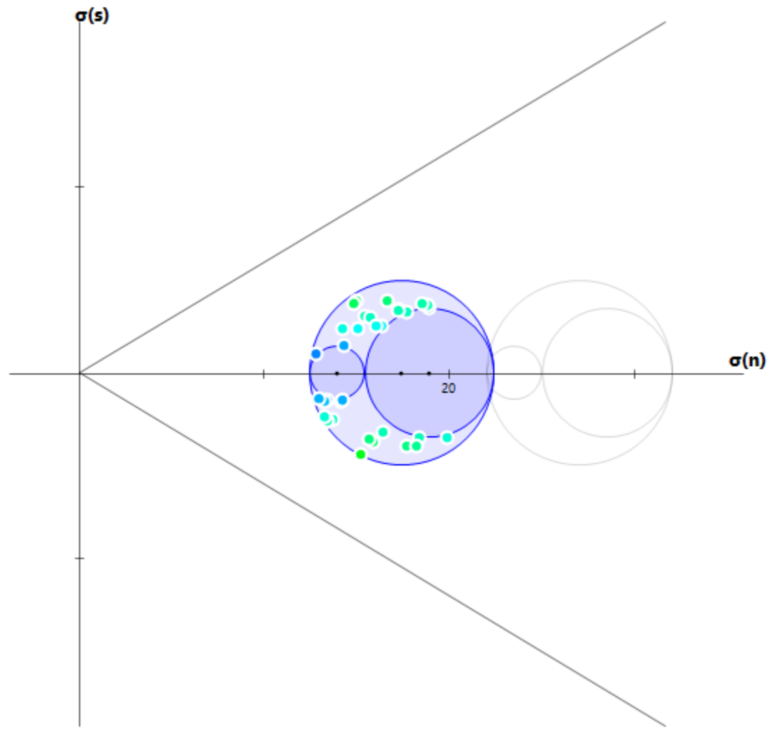

Figure 31. Mohr diagram for fractures identified in well 100/05-03-082-18W6/00. Inputs: S_{hmin} = 44 MPa, S_V = 50 MPa, S_{Hmax} = 64 MPa, P_P = 19.2 MPa.

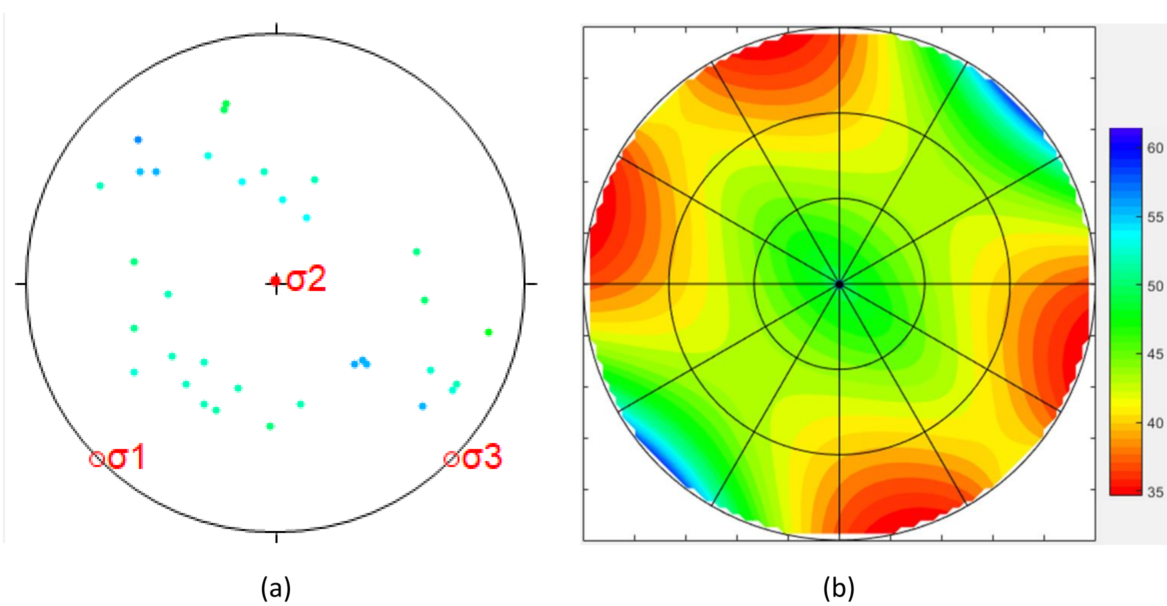

Figure 32. Stereonets for well 100/05-03-082-18W6/00. [Note colours in a do not directly correspond to colours in b]

VII. Summary and Recommendations

Key Findings

The KSMMA and surrounding area are in the heart of the region recording the longest period of tectonic activity in the Western Canada Sedimentary Basin. Beginning with uplift in the Proterozoic, most likely through reverse faulting, the Study Area remained a positive feature until the Early Carboniferous at which time it began to collapse through a series of normal faults. This faulting decreased towards an infill phase at the end of the Permian. Evidence of strike-slip faulting began to be experienced during the Triassic, particularly in the northern part of the study area. The onset of the Columbia Orogeny and associated compression during the Jurassic marked the transition of the normal and strike-slip faults to a transpressional setting. This compression enhanced during the Laramide Orogeny. The most significant post-Laramide tectonic event was the crustal loading during the Laurentide Glaciation and subsequent isostatic rebound due to erosional unroofing and melting of the Cordilleran Ice Sheet. This rebound has been estimated to be approximately 4 mm/year in the Study Area.

Public domain pressure data for the Debolt through Triassic interval was collated and processed for quality control. As with all Montney related data in this study, the pressure data was correlated to a widely accepted stratigraphic model of Upper, Middle and Lower Montney. The Debolt through Belloy interval, considered to be in a conventional normally pressured setting, displayed a significant number of over-pressured data points. While previous exploration was predicated on the concept of sealing and non-sealing faults, the presence of over-pressuring related to these features is anomalous. The Upper and Middle Montney displayed a similar compartmentalization of pressures with down dip and along strike variations in pore pressure gradient. These pressure variations have a strong correlation with the significant and well documented faults in the study area and outline a series of interpreted Pressure Terranes. The NRCan events show a propensity to cluster in the proximity the boundaries between a number of these terranes.

Based on our current modeling, the state of stress throughout much of the KSMMA at depths between the Doig and Belloy is strike-slip and in a near critical state, meaning only small fluid pressure increases are sufficient to cause the most critically oriented fractures and faults to become critically stressed. The amount of pressure needed is closely tied to the existing formation pressure – areas with higher natural pressures require lower pressure increases. Fractures/faults that will become critically stressed first, if they exist, strike approximately 15° to 45° from the northeast-southwest S_{Hmax} orientation and are dipping more than 60°. Further study is needed to better understand both the state of stress and the distribution of existing faults and fractures in the KSMMA, as well as the implications of the discrepancy between the known seismic events and the most critically stressed fracture/fault orientations and their relationship to Montney stratigraphy.

Recommendations

While identifying all existing subsurface faults will likely always remain challenging, there is a substantial existing dataset that has not been used to its full potential. The same comment applies to determining the local stress field. Once the latter is achieved, the workflow for analyzing the mechanical stability of real and hypothetical fractures and faults is well-established and has been followed in this study.

The limitations in our current understanding of induced seismicity in the KSMMA are primarily based on two things: data and time. Access to data, as well as data quality, remain key challenges in the study area. This has been addressed in each of the report sections.

Once data issues are sorted out, it will take significantly more time and expertise to fully analyze the full data set. Many of the tasks that are needed are discussed this section. While extensive, the list is not exhaustive. As insights regarding induced seismicity are made elsewhere in the world, the KSMMA may need to be looked at with a new perspective.

Minifrac Data

Diagnostic Fracture Injection Tests (DFITs) are the primary source for determining minimum principal stress magnitude and are rapidly becoming a primary source of reservoir pressure data. These tests have not been interpreted to a consistent level of quality and rigour. Our recommendations include:

1. Create a database of minifrac data across the KSMMA and buffer
2. Apply a consistent interpretation approach for both minimum stress and formation pressure
3. Develop a Quality Code ranking and apply to each minifrac
4. Define consistent submission guidelines

Structural Analysis

While establishing the regional structural framework was critical in the area seismicity, a detailed understanding of the structuring within the KSMMA will be part of fine tuning the regulatory response to seismicity concerns. This can be accomplished using all available data types such as 3D seismic. Our recommendations include:

1. Create a detailed structural interpretation for key stratigraphic intervals (e. g. Wabamun, Debolt, Belloy, Montney and Halfway)
2. Classify faulting by structural style, orientation and dip
3. Investigate the timing and magnitude of North Pine salt solution as a proxy for seismicity

In the future, further study into the potential role of deglaciation and overburden removal on seismicity risk may be beneficial, in which case we recommend the following:

1. Apply thermal gradient values and petrophysical techniques to enhance estimate of overburden removal
2. Model the effects of removal of the Laurentide ice sheet
3. Verify glacial rebound rate using, e.g., synthetic aperture radar interferometry (INSAR)

Hydrodynamics Analysis

Variations in pressure are important to understanding the causes of induced seismicity and the effects of introduced pressure on critically stressed faults. The current understanding can be enhanced by focussing on variations in the KSMMA. These steps can include:

1. Use the enhanced pore pressure data from the minifracs to expand the hydrodynamic interpretation of the KSMMA area. Goals include refining the pressure terrane boundaries, differentiating terranes within the Montney stratigraphy and identification of pressure leakage points and areas with anomalous pressures
2. Add new pressure data types – e.g., gas readings, kicks/inflows from daily drilling reports
3. Further the pressure compartmentalization story (e.g., Finkbeiner et al., 2001)

© 2019 Enlighten Geoscience Ltd.

4. Evaluate hydrodynamic setting of the post-Montney Triassic, if seismic events are identified within these intervals

Geomechanical Interpretation

Geomechanical characterization of an area is one of the most important steps towards mitigating induced seismicity (Walters et al., 2015). Image logs are critical for determining the magnitude and orientation of the maximum horizontal stress, as well as for identify fractures and faults, but the application of this tool is seriously limited by issues regarding quality, availability and sampling bias. Currently images range from good quality, colour versions of wellbore images to uninterpretable black and white versions, if they are available at all. Our recommendations with respect to image logs include:

1. For existing images, obtain high quality versions from operators if they have not already submitted them
2. Perform a consistent interpretation for natural fractures and faults (including interpreting bedding dips for structures/faults) using all the image logs
3. For new wells, revise image log submission guidelines so that the image submitted is always the final, processed, oriented data at reasonable vertical scales for interpretation. Specify whether interpretations are required to be submitted if they are performed, and in what format (e.g., text files of feature picks)

Once image logs have been consistently analyzed for natural fractures and faults, a structural analysis could be performed to determine relationship to structure, potential for connectivity, size distribution, etc.

In order to complete the geomechanical interpretation, the following tasks should be performed:

1. Determine stress magnitudes in as many wells as possible
2. Map stress orientations from all available data types (image logs, oriented caliper logs, sonic anisotropy/scanner logs)
3. Perform critically stressed fracture analysis on the consistently picked fractures/faults

Numerous rock mechanics tests have been performed on Montney core in the KSMMA area, but most of the time the testing programs were not designed to capture strength properties. Also, most were in the Montney where almost no failure is observed. We recommend that new testing programs could be undertaken on existing core to better constrain UCS and other important parameters like friction angle in formations where stress-induced failure is observed. Tests can also be performed to try to estimate the frictional strength of pre-existing fractures, which is a major unknown in Mohr-Coulomb analysis for fault slip.

It should be noted that there are additional data types that could be used to try to characterize the natural fracture/fault populations and stress state. These include microseismic data collected during stimulations, passive microseismic and tomographic fracture imaging (Lacazette and Morris, 2015; Geiser, 2012), core photos (or the cores themselves), detailed drilling data, and stress rotations.

Completions Review, Statistical Analysis and Hydraulic Fracture Modeling

Numerous authors have attempted to link operational parameters during hydraulic fracturing to induced seismicity (e.g., Norbeck and Horne, 2018; Shultz et al., 2018). Although it is early in our understanding of the role of parameters such as volume, rates and pressures, it is likely that there is one. This is likely the case at least in some plays/areas, even if it is in combination with geological parameters such as higher or lower formation pressures and fault orientations or frictional strength.

Given the extensive data set of hydraulically fractured completions in the study area, it would likely be an informative, if labour-intensive, exercise to try to find a correlation between operational parameters and induced events in the KSMMA. The application of recursive partitioning and other multivariate statistical techniques to determine relationships between various completion practices (e.g. pumping pressure, proppant tonnage, fluid rate), geological factors (e.g. fault orientation and dip, critically stressed fault orientation, S_{HMax} orientation, pressure gradient transitions) with frequency and magnitude of induced seismicity events could be explored for this purpose.

Another potentially insightful study could include using improved data on natural fractures and faults present in the Montney and surrounding formations to perform exploratory modeling which would examine the interaction between hydraulic and natural fractures (Rogers, 2018).

VIII. References

Almendinger, R. W., MohrPlotter v. 2.8, 2015

Allen, D. M., E. Eberhardt and A. Bustin, Scientific Review of Hydraulic Fracturing in British Columbia, February 2019 [link]

Anderson, E. M., Dynamics of Faulting and Dyke Formation with Application to Britain, 2nd ed. Edinburgh: Oliver and Boyd, 183 p., 1951

Barclay, J. E., F. F. Krause, R. I. Campbell and J. Utting, Dynamic casting of a graben complex: Basin infill and differential subsidence during the Permo-Carboniferous; Peace River Embayment, Western Canada. Bulletin of Canadian Petroleum Geology, v. 38A, p. 115-145, 1990

BC Oil & Gas Commission, Pool Breaklines Shapefiles, 2019 [link]

BC Oil and Gas Commission, Industry Bulletin 2018-09, New Seismic Monitoring Plans Required for Operators in Farmington, May 14, 2018

Burwash, R. A., C. R. McGregor and J. A. Wilson, Precambrian basement beneath the Western Canada Sedimentary Basin. In: Geological Atlas of the Western Canada Sedimentary Basin. G.D. Mossop and I. Shetsen (comps.). Calgary, Canadian Society of Petroleum Geologists and Alberta Research Council, ch. 5, 1994 [link]

Davies, G., N. Watson, T. Moslow and J. MacEachern, Regional Subdivisions, Sequences, Correlations and Facies Relationships of the Lower Triassic Montney Formation, West-Central Alberta to Northeastern British Columbia, Canada — with Emphasis on Role of Paleostructure, Bulletin of Canadian Petroleum Geology, v. 66, n. 1, p. 23-92, 2018

Dixon, J., A review of the character and interpreted origins of thick, mudstone-encased sandstone bodies in the Middle Triassic Doig Formation of Western Canada, Bulletin of Canadian Petroleum Geology vol. 59, n. 3, p. 261–276, 2011

Graham Davies Geological Consultants (GDGC) Ltd. and A. Hamid Majid, The Mississippian Debolt Project Northeastern British Columbia Phase 1, 1990

Dawson, F. M., C. G. Evans, R. Marsh and R. Richardson, Uppermost Cretaceous and Tertiary strata of the Western Canada Sedimentary Basin. In: Geological Atlas of the Western Canada Sedimentary Basin. G.D. Mossop and I. Shetsen (comps.). Calgary, Canadian Society of Petroleum Geologists and Alberta Research Council, ch. 24, 1994 [link]

Earthquakes Canada (Natural Resources Canada), National Earthquake Database, 2018 [link]

Ellsworth, B., C. Langenbruch, J-E. Lund-Snee, M. Schoenball, C. Yoon, M. Weingarten, G. Beroza and M. Zoback, Induced Earthquakes: State of the Science 2018, Banff 2018 International Induced Seismicity Workshop, October 24-26, 2018, Banff, Alberta, Canada, 2018

Euzan, T., T. Moslow, V. Crombez and S. Rohais, Regional Stratigraphic Architecture of the Spathian Deposits in Western Canada — Implications for the Montney Resource Play, Bulletin of Canadian Petroleum Geology. v. 66, n. 1, p. 175-192, 2018

Geiser, P., A. Lacazette and J. Vermilye, Beyond ‘dots in a box’: an empirical view of reservoir permeability with tomographic fracture imaging, First Break, v. 30, p. 63-69, 2012

Finkbeiner, T., M. Zoback, P. Flemings and B. Stump, Stress, pore pressure and dynamically constrained hydrocarbon columns in the South Eugene Island 330 field, northern Gulf of Mexico, AAPG Bulletin, v. 85, n. 6, pp. 1007-1031, 2001

Gillen, K., Fracture Study of the Montney Formation from ECA HZ Tower C16-6-81-17, N.E. British Columbia, Canada, for Encana Corporation, 2017

Grasby, S.E., D.M. Allen, S. Bell, Z. Chen, G. Ferguson, A. Jessop, M. Kelman, M. Ko, J. Majorowicz, M. Moore, J. Raymond and R. Therrien, Geothermal Energy Resource Potential of Canada, Geological Survey of Canada Open File 6914, 2012

Grollimund, B. and M.D. Zoback, Did deglaciation trigger intraplate seismicity in the New Madrid seismic zone?, Geology, v. 29, n. 2, p. 175-178, 2001

Hayes, B.J.R., S. Macleod and J. Carey, Characterization of Belloy, Kiskatinaw and Debolt water disposal zones in the Montney play area, northeastern British Columbia; in Geoscience BC Summary of Activities 2014, Geoscience BC, Report 2015-1, p. 85–88, 2015 [link]

Heidbach, O., M. Rajabi, X. Cui, K. Fuchs, B. Müller, J. Reinecker, K. Reiter, M. Tingay, F. Wenzel, F. Xie, M. O. Ziegler, M.-L. Zoback, and M. D. Zoback, The World Stress Map database release 2016: Crustal stress pattern across scales. Tectonophysics, 744, 484-498, doi:10.1016/j.tecto.2018.07.007, 2018

Heidbach, Oliver; Rajabi, Mojtaba; Reiter, Karsten; Ziegler, Moritz; WSM Team: World Stress Map Database Release 2016. GFZ Data Services, doi:10.5880/WSM.2016.001, 2016

Huang, L. and C.-y. Liu, Three types of flower structures in a divergent-wrench fault zone. Journal of Geophysical Research: Solid Earth, 122, 2017 [link]

Jamison, W., Thin section examination of deformational features developed in Doig Phosphate, for Shell Canada, 2011

© 2019 Enlighten Geoscience Ltd.

Khaksar, A., P.G. Taylor, Z. Fang, T. Kayes, A. Salazar and K. Rahman, Rock Strength from Core and Logs: Where We Stand and Ways to Go, SPE 121972, 2009

Koohzare, A., P. Vanıcek and M. Santos, Pattern of recent vertical crustal movements in Canada. Journal of Geodynamics v. 45, p. 133–145, 2008 [link]

Lacazette, A. and A. Morris, A New Method of Neostress Determination from Passive Seismic Data, Unconventional Resources Technology Conference (URTeC) DOI 10.15530/urtec-2015-2174187, 2015

Leckie, D., M. Staniland and B. Hayes, Regional Maps of the Albian Peace River and Lower Shaftesbury Formations on The Peace River Arch, Northwestern Alberta and Northeastern British Columbia, Bulletin of Canadian Petroleum Geology, v. 38A, n. 1, p. 176-189, 1990

Lund Snee, J.-E. and M. D. Zoback, State of Stress in the Permian Basin, Texas and New Mexico: Implications for induced seismicity, The Leading Edge, Feb, p. 127, 2018

Moslow, T., B. Haverslew and C. Henderson, Sedimentary Facies, Petrology, Reservoir Characteristics, Conodont Biostratigraphy and Sequence Stratigraphic Framework of a Continuous (395m) Full Diameter Core of the Lower Triassic Montney Fm, Northeastern British Columbia. Bulletin of Canadian Petroleum Geology. v. 66, n. 1, p. 259-287, 2018

Ngo, D. T., F. L. Pellet and D. Bruel, Modeling of fault slip during hydraulic fracture stimulation in a naturally fractured medium, Geomechanics and Geophysics for Geo-Energy and Geo-Resources, 2019 [link]

Norbeck, J. H. and R. N. Horne, Maximum magnitude of injection-induced earthquakes: A criterion to assess the influence of pressure migration along faults, Tectonophysics, v. 733, p. 108-118, 2018

Norgaard, G., Structural inversion of the Middle Triassic Halfway Formation, Monias Field, northeast British Columbia, 1997

O'Connell, S.C., The development of the Lower Carboniferous Peace River Embayment as determined from Banff and Pekisko formation depositional patterns, Bulletin of Canadian Petroleum Geology, v. 38A, p. 93-114, 1990

O'Connell, S.C., Geological history of the Peace River Arch. In: Geological Atlas of the Western Canada Sedimentary Basin. G.D. Mossop and I. Shetsen (comps.). Calgary, Canadian Society of Petroleum Geologists and Alberta Research Council, ch. 28, 1994 [link]

Ragan, D., 1973. Structural Geology: An Introduction to Geometrical Techniques. Cambridge University Press.

Rogers, S., What Can Discrete Fracture Network Analysis Tell Us About Induced Seismicity in the Montney Formation?, GeoConvention abstract, 2018

Ross, G. M., J. Broome and W. Miles, Potential fields and basement structure - Western Canada Sedimentary Basin. In: Geological Atlas of the Western Canada Sedimentary Basin. G.D. Mossop and I. Shetsen (comps.). Calgary, Canadian Society of Petroleum Geologists and Alberta Research Council, ch. 4, 1994 [link]

Shultz, R., G. Atkinson, D.W. Eaton, Y. J. Gu and H. Kao, Hydraulic fracturing volume is associated with induced earthquake productivity in the Duvernay play, Science, v. 359, p. 304-308, 2018

USGS, https://www.usgs.gov/faqs/what-a-fault-and-what-are-different-types?qt-news_science_products=0#qt-news_science_products, 2019a

USGS, https://earthquake.usgs.gov/earthquakes/eventpage/us1000hy6d/moment-tensor?source=us&code=us_1000hy6d_mwr, 2019b

Walters, R. J., M. D. Zoback, J. W. Baker and G. C. Beroza, Scientific Principles Affecting Protocols for Site-characterization and Risk Assessment Related to the Potential for Seismicity Triggered by Saltwater Disposal and Hydraulic Fracturing, Stanford Center for Induced and Triggered Seismicity, 2015 [link]

Zoback, M.D., Reservoir Geomechanics, 2nd Ed., Cambridge University Press, 2010

Zonneveld, J.-P. and T. Moslow, T., Palaeogeographic Setting, Lithostratigraphy, and Sedimentary Framework of the Lower Triassic Montney Formation of Western Alberta and Northeastern British Columbia, Bulletin of Canadian Petroleum Geology. v. 66, n. 1, p. 93-127, 2018

IX. Appendices

The appendices are available as separate documents.

Appendix A: Geophysical Review

Appendix B: Minifrac Review

Appendix C: Figures and Enclosures

Appendix D: Mapping and Pressure Data Files

© 2019 Enlighten Geoscience Ltd.